

Article

COSMC-Regulated O-Glycosylation: A Bioinformatics-Driven Biomarker Identification for Stratifying Glioblastoma Stem Cell Subtypes

Sara Sadat Aghamiri and Rada Amin *

Department of Biochemistry, University of Nebraska, Lincoln, NE 68503, USA

* Correspondence: raminali2@unl.edu or rada.aminali@gmail.com

Abstract: Glioblastoma stem cells (GSCs) are key drivers of relapse, metastasis, and therapy resistance in glioblastoma due to their adaptability and diversity, which make them challenging to target effectively. This study explores the O-glycosylation in differentiating two key GSC subtypes, CD133 and CD44. We utilized the TCGA dataset of GBM and presented the reproducible bioinformatics analysis for our results. Our profiling showed enriched O-glycosylation signatures in CD44-expressing GBM cells over CD133, with *Cosmc*, the chaperone for core mucin-type O-glycosylation, significantly up-regulated in the CD44-positive group. Moreover, *Cosmc* was associated with shorter progression-free intervals, suggesting its potential as an indicator of aggressive disease. High *Cosmc* expression also enriched immune-related pathways, including inflammatory response and antigen presentation, and was associated with presence of myeloid cells, T cells, and NK cells. Additionally, elevated *Cosmc* correlated with extracellular matrix (ECM) pathways and stromal cell populations, such as perivascular fibroblasts. These findings position O-glycosylation, specially, *Cosmc* as a promising biomarker for distinguishing GSC subclones, with relevance to immune modulation, and ECM dynamics, identifying it as a potential target for novel GBM therapies.

Keywords: cancer stem cells; glioblastoma; O-glycosylation; *Cosmc*; CD44; CD133



Citation: Aghamiri, S.S.; Amin, R. COSMC-Regulated O-Glycosylation: A Bioinformatics-Driven Biomarker Identification for Stratifying Glioblastoma Stem Cell Subtypes. *Kinases Phosphatases* **2024**, *2*, 391–412. <https://doi.org/10.3390/kinasesphosphatases2040025>

Academic Editor: Mauro Salvi

Received: 12 November 2024

Revised: 17 December 2024

Accepted: 19 December 2024

Published: 22 December 2024



Copyright: © 2024 by the authors. Licensee MDPI, Basel, Switzerland. This article is an open access article distributed under the terms and conditions of the Creative Commons Attribution (CC BY) license (<https://creativecommons.org/licenses/by/4.0/>).

1. Introduction

Glioblastoma (GBM) poses a significant challenge in modern therapy, due to its rapid progression, invasiveness, and resistance to standard treatments, including surgery, radiation, and chemotherapy [1]. A key contributor to this disease's persistence is a rare subset of cells known as glioblastoma stem cells (GSCs), which drive tumor growth, recurrence, and resistance to conventional therapies [2,3]. GSCs possess plasticity, self-renewal, and pluripotency, enabling them to repopulate the tumor even after apparent tumor clearance. This resilience is largely due to their ability to adapt to environmental pressures through dynamic signaling reprogramming [4]. Two primary surface markers, CD133 and CD44, are commonly used to identify GSCs. CD133, a cell surface glycoprotein, is frequently expressed in GSCs and is associated with enhanced tumorigenicity and resistance to therapy [5,6]. CD44, a receptor involved in cell–cell and cell–matrix interactions, marks a subset of mesenchymal glioma stem cells and is linked to invasive behavior [7]. Despite advances in our understanding of GSCs, there is still no clear consensus on their heterogeneity, distribution within tumors, or the hierarchy of sub-clones contributing to tumoral diversity [8]. For instance, hypoxic conditions induce a shift from CD44+ to CD133+ cells, while chemotherapy triggers the reverse transition [9]. Furthermore, CD133- cells display stem cell-like properties yet exhibit distinct proliferative and molecular programming, reflecting the diversity in GSC origin and subtypes [10].

Additionally, CSCs actively shape the tumor microenvironment by recruiting a diverse array of immune and stromal cells with specialized functions that support GSC survival and maintenance [11,12]. These recruited cells establish a unique microenvironment, known

as the tumor niche, which supplies GSCs with essential signaling molecules, nutrients, and immune protection. This supportive interaction enhances GSC survival, self-renewal, and resistance to therapies and tumor progression. Together, these interactions contribute to the tumor's resilience and therapy resistance, ultimately leading to a poor prognosis for patients [13]. Identifying novel markers to differentiate GSC subclones within GBM's heterogeneous landscape is essential; such markers could not only improve our understanding of GBM biology, but also guide the development of targeted therapies that selectively eliminate cancer stem cells (CSCs), and potentially reduce recurrence.

Aberrant glycosylation is a hallmark of cancer, frequently used by CSCs to facilitate immune evasion, stemness, proliferation, survival, drug resistance, and metastasis [14–17]. Specifically, O-glycosylation, where sugars attach to the oxygen atom on serine or threonine residues, modulates cell surface proteins critical for immune modulation and tumor growth [18–20]. Dysregulated O-glycosylation in cancer has been associated with the invasive and stem-like properties of CSCs, highlighting its potential as a target for understanding GBM progression and developing therapies [21]. For instance, disruption of core 1-mediated O-glycosylation reduces CD44 expression on the cell surface and increases its exosomal release in colon cancer, whereas restoring *Cosmc* (core 1 β 3GalT-specific molecular chaperone) rescues CD44 surface expression [22]. Similarly, truncated O-glycans on CD44 enhance stemness properties in pancreatic cancer [23]. In GBM, inhibition of GALNT2, an enzyme that initiates mucin-type O-glycosylation, suppresses self-renewal in vitro and in vivo by downregulating CD44 expression [24]. These studies indicate that a proper O-glycosylation pathway is necessary for CD44 integrity and functionality. Overall, O-glycosylation is a conserved mechanism across cancers for maintaining CSC stemness properties, particularly in GBM.

In this study, we identified differential O-glycosylation patterns in CD133- and CD44-expressing groups, focusing on *Cosmc* as a key molecule. Our bioinformatic analysis of TCGA data revealed that elevated *Cosmc* expression was associated with shorter progression-free survival, highlighting its potential as a therapeutic target. Notably, *Cosmc* was predominantly showing correlations with immune and stromal activity, inflammatory pathways, immunosuppressive environments, and ECM remodeling. By investigating the role of O-glycosylation markers like CD44 and CD133 associated with GSCs, we aim to determine whether O-glycosylation distinguishes CD133- and CD44-stem-like cells, and how it contributes to the complex cellular interactions within the TME.

2. Results

2.1. Distinct O-Glycosylation Signatures in CD44 and CD133 Subtypes of GBM Reveal Prognostic Potential of COSMC

We first evaluated O-glycosylation signatures in GBM patients expressing CD44 and CD133 groups, using TCGA data. Our results showed that the CD44 group was significantly enriched in several O-glycosylation signatures, with the strongest association observed for DISEASES_OF_GLYCOSYLATION ($p = 0.008$). Conversely, the CD133 group displayed downregulation in only one significant pathway: O_LINKED_GLYCOSYLATION_OF_MUCINS ($p = 0.006$) (Figure 1A). An inverse pattern in O_LINKED_GLYCOSYLATION_OF_MUCINS was noted between the CD44 ($p = 0.047$) and CD133 groups ($p = 0.0063$). To identify genes specific to mucin-related signaling, we performed an intersection analysis of gene sets linked to CD44 and CD133. This analysis revealed 14 common genes, while 6 were unique to CD44 and 8 to CD133 (Figure 1B). We then focused on these unique genes for each marker, comparing their expression in GBM versus normal brain tissue (Figure 1C). In the CD133 group, GALNT9 and GCNT4 were significantly downregulated, while ST6GAL1 was upregulated in GBM. In the CD44 group, B3GNT5 and *Cosmc* (C1GALT1C1) were upregulated in GBM compared to normal tissue (Figure 1D). To assess the prognostic value of these genes, we used the Xena platform to analyze overall survival (OS) and progression-free interval (PFI). This analysis indicated a significant association between *Cosmc* expression and PFI ($p = 0.0091$) (Figure 1E). To further explore the relationship

between *Cosmc* and CD44, we analyzed the Ivy Glioblastoma Atlas Project (Ivy-GAP) cohort to assess the spatial associations between these two markers. Our analysis revealed a significant correlation between *Cosmc* and CD44 (Appendix A, Figure A1A), but not with CD133 (Appendix A, Figure A1B). Additionally, we examined other datasets to evaluate the distribution of *Cosmc* in CD133⁻/CD133⁺ and CD44⁻/CD44⁺ GBM. For this, we selected one dataset in which CSCs were sorted based on CD133 markers (GSE85297) and one dataset in which GBM cells were also isolated, based on CD133 (GSE34152). Both datasets showed no significant difference in *Cosmc* expression in CD133⁻ and CD133⁺ populations (Appendix A, Figure A1C,D). Next, we selected an RNA-sequencing dataset and stratified the samples into CD133⁻/CD133⁺ and CD44⁻/CD44⁺ groups based on the median expression levels of CD133 and CD44, respectively, then assessed *Cosmc* gene expression. Our analysis showed that *Cosmc* was significantly enriched in the CD44⁺ group compared to the CD44⁻ group, while no significant differences were observed between the CD133 groups (Appendix A, Figure A1E). Our findings highlight distinct O-glycosylation patterns in GBM associated with CD44 and CD133 expression, revealing unique gene signatures and suggesting a prognostic role for *Cosmc*.

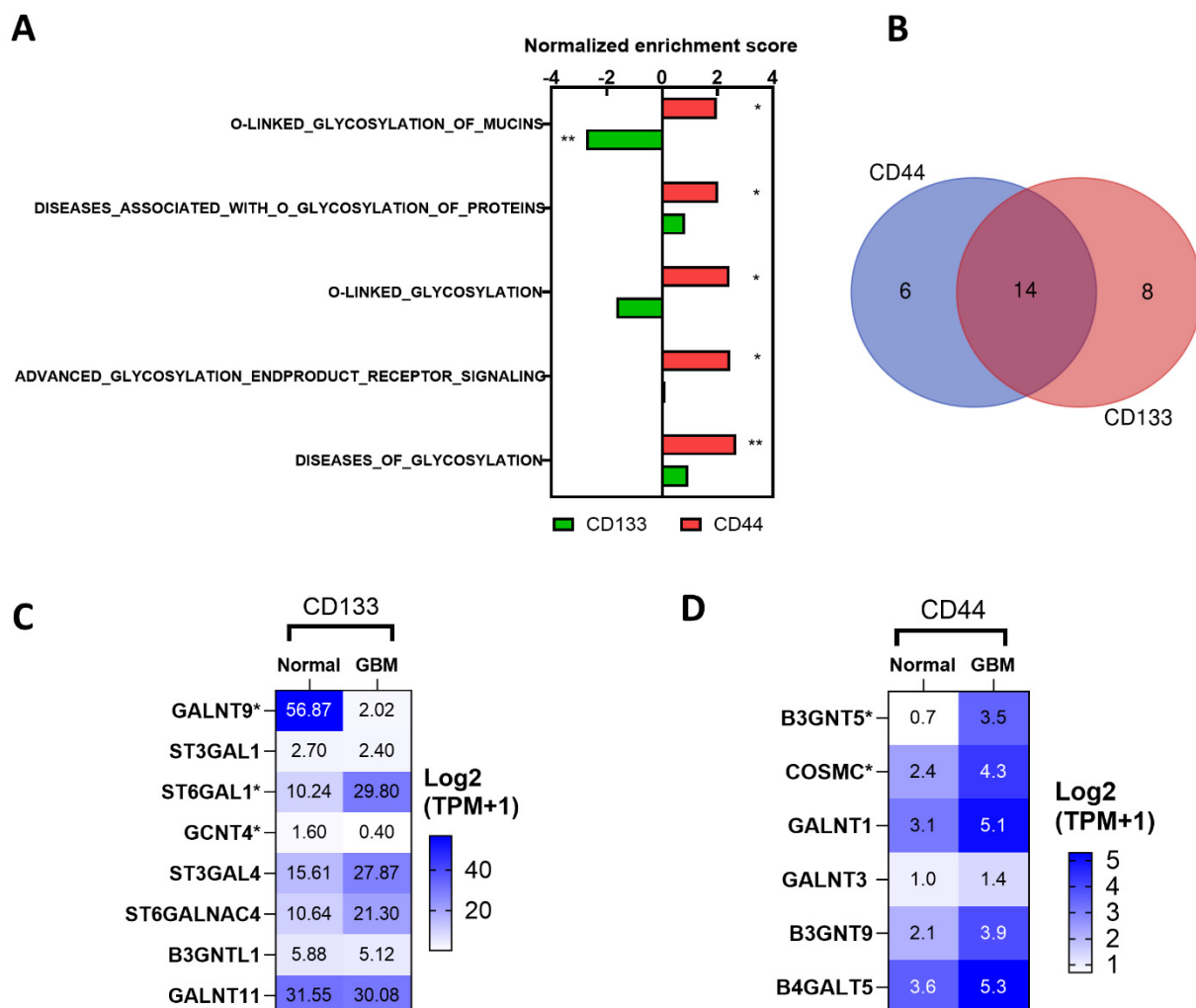


Figure 1. Cont.

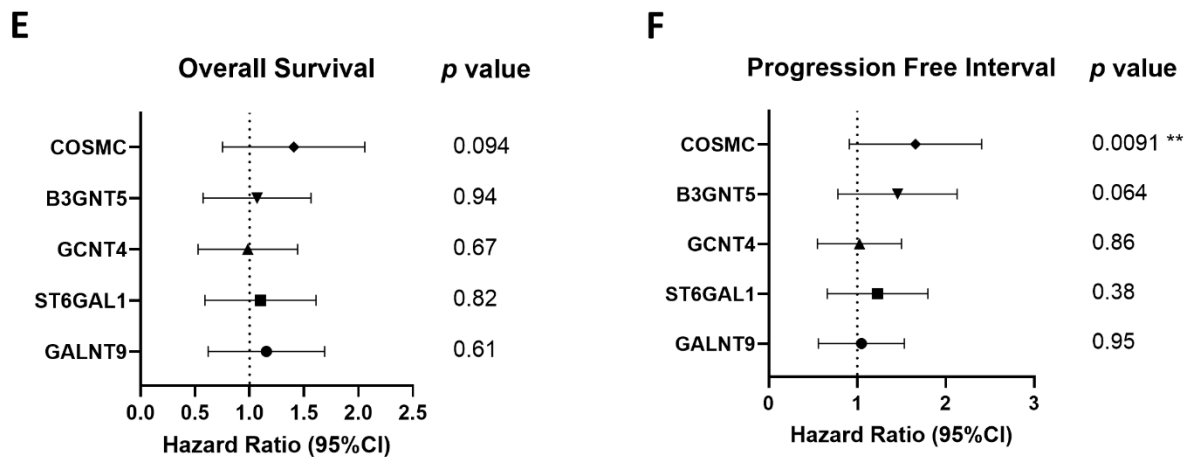


Figure 1. COSMC is associated with the CD44 GBM stem cell marker, but not with CD133. (A) The O-glycosylation-related pathways enriched in CD44 (red) and CD133 (green), with a p -value shown. * $p < 0.05$, ** $p < 0.01$. (B) The C Venn diagram represents the shared and unique gene number among the O-linked_glycosylation_Of_Mucins in the CD44 and CD133 groups. (C) The log₂ normalized TPM median gene expression of 8 genes in the CD133 group compared to normal brain tissue within Gepia, * $p < 0.05$. (D) The log₂ normalized TPM median gene expression of 6 genes in the CD44 group compared to normal brain tissue within Gepia. The statistical test was performed using one-way ANOVA, * $p < 0.05$. (E) Forest plot of overall survival of the significant overexpressed genes among both CD133 and CD44 groups. (F) Forest plot of progression-free interval of the significant overexpressed genes among both CD133 and CD44 groups. The statistical test was performed using the log rank test, ** $p < 0.01$.

2.2. COSMC-C1GALT1-ST3GAL1 Chain in Glioblastoma Shows Links to CD44

While *Cosmc* dysfunction has been identified in several diseases, including solid cancers, its specific role and impact with regard to GBM remain largely unexplored [25]. During mucin type O-glycan biosynthesis, *Cosmc* facilitates C1GALT1 (core 1 β 1,3-galactosyltransferase) proper folding and stability, essential for synthesizing mucin-type O-glycans. With *Cosmc* support, C1GALT1 processes the Tn antigen (GalNAc α 1-Ser/Thr-R) to form core 1 Gal β 1-3GalNAc α 1-Ser/Thr (T antigen) and prevents the accumulation of the Tn antigen [26]. Downstream, ST3GAL1 and B3GNT3 further modify these glycan structures by adding sialic acid and N-acetylglucosamine, respectively, influencing the diversity and functionality of glycoproteins [27] (Figure 2A). To investigate the association of these glycan chains with CD44 and CD133, we first compared C1GALT1, ST3GAL1, and B3GNT3 expression in GBM and normal brain tissue. Notably, both *Cosmc* (Figure 1D) and C1GALT1 showed significant upregulation in GBM, whereas ST3GAL1 did not show statistically significant differences (Figure 2B). B3GNT3 gene expression was not significantly detected. We then assessed correlations between these genes and the markers CD44 and CD133. Spearman correlation analysis revealed a positive association between CD44 and both C1GALT1 and ST3GAL1, with no significant association for B3GNT3. Conversely, CD133 was negatively correlated with ST3GAL1, and showed no significant correlation with C1GALT1 or B3GNT3 (Figure 2C). Finally, we evaluated the prognostic relevance of these genes in GBM. We could not assess B3GNT3 clinical association because it did not have significant enough cohort size to perform the analysis; therefore, we could only perform this analysis for C1GALT1 and ST3GAL1. Our findings indicated that none of the genes exhibited clinical significance for GBM prognosis (Figure 2C). Overall, our analysis highlights a positive association between the COSMC-C1GALT1-ST3GAL1 chain and CD44, with *Cosmc* being the only component showing clinical relevance.

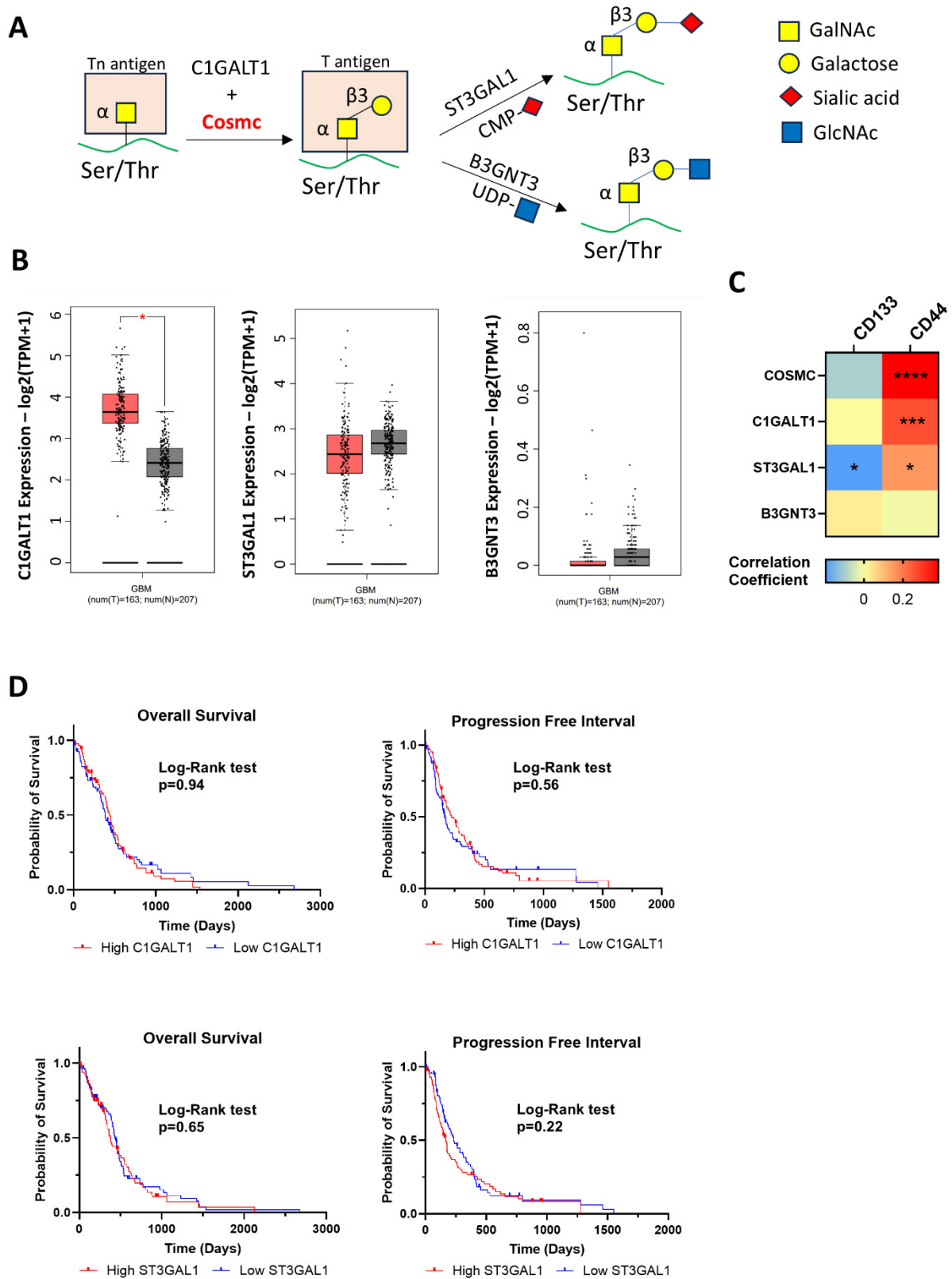


Figure 2. O-glycosylation core pathways in GBM. (A) Cosmc O-glycosylation model, GalNAc, N-acetylgalactosamine, GlcNAc, N-acetylglucosamine. (B) Gene expression of C1GALT1, ST3GAL1 and B3GNT3 compared in matched normal brain versus GBM. Statistical test was performed using one-way ANOVA, * $p < 0.05$. (C) Heatmap displaying the Spearman correlation between the O-glycosylation core with CD133 and CD44. Statistical test was performed with Spearman correlation

test, and the significant p value was displayed on the heatmap. **** $p < 0.0001$, *** $p < 0.001$, * $p < 0.05$. (D) Kaplan–Meier curve of overall and progression-free survival analysis of C1GALT1, ST3GAL1, with code color as follows: high (red) and low expression (blue). The difference between the two curves were determined by the two-sided log-rank test.

2.3. COSMC Is Significantly Correlated with Mesenchymal Stem-like Phenotype

To further explore the relationship between *Cosmc* and GSCs, we focused on assessing the enrichment of stem cell-related pathways by comparing groups with high ($n = 86$) and low ($n = 86$) *Cosmc* expression, based on the median expression. Gene set enrichment analysis (GSEA) revealed significant enrichment of multiple stem cell signaling pathways in GBM, including *NRF2* ($p < 0.0001$) [28], *integrin 3* ($p = 0.00087$) [29], *CXCR4* ($p = 0.0061$) [30], *uPA-uPAR* ($p = 0.0063$) [31], *RUNX1* ($p = 0.011$) [32], and *PPAR* ($p = 0.015$) [33] (Figure 3A). Additionally, we observed enrichment of canonical pathways linked to stemness, such as stem cell pathways ($p = 0.012$), hematopoietic stem cell differentiation ($p = 0.03$), and pluripotent stem cell differentiation ($p = 0.049$).

To quantify the association between *Cosmc* and stem cell markers, we applied gene set variation analysis (GSVA), scoring a curated gene set comprising *NRF2*, *integrin 3-ITGAV*, *CXCR4*, *uPA*, *uPAR*, *RUNX1*, and *PPARG*. This provided an estimated activity level for stemness-related pathways. Correlation analysis further indicated a significant association between *Cosmc* and these gene sets, reinforcing the relevance of *Cosmc* in stem cell signaling within GBM (Figure 3B). To further validate the association between *Cosmc* and the stemness phenotype, we analyzed additional cohorts, including the Repository of Molecular Brain Neoplasia Data (Rembrandt) and the Gravendeel dataset. We first compared *Cosmc* gene expression of normal brain tissue and GBM across both cohorts, and observed significantly elevated *Cosmc* expression in GBM in both datasets (Appendix A, Figure A2A,B). We then assessed the individual correlations between *Cosmc* and various stem cell genes. The results demonstrated a generally strong correlation between *Cosmc* and each stem cell gene, with the exception of *RUNX1* in the Gravendeel cohort (Appendix A, Figure A2C).

The GSCs have been observed to reside in a quiescent, or slow-cycling, state [34]. Additionally, Brown et al. reported that CD133-positive GSCs are more proliferative, while CD44-positive GSCs exhibit a more quiescent phenotype [9]. To examine this in the context of *Cosmc*, we analyzed hallmark pathways enriched in *Cosmc*-high groups. Our results indicated a downregulation of cell cycle-related pathways, including the G2M checkpoint, mitotic spindle assembly, and E2F target regulation (Figure 3C). In contrast, upregulated pathways included those involved in inflammatory response, $\text{IFN}\gamma$ signaling, metabolism, cytokine signaling, apoptosis, coagulation, and hypoxia (Figure 3C). Interestingly, the enrichment analysis showed an upregulation of epithelial–mesenchymal transition pathways (EMT), which is often related to stemness and aggressive behavior of GBM [35] (Figure 3C).

To further investigate the association of *Cosmc* with a slow-cycling phenotype, we assessed its correlation with genes linked to both slow- and fast-cycling states. Specifically, we analyzed its relationship with genes associated with cycling that have been investigated in GBM. We selected three fast-cycling genes, *CDK2* (cyclin-dependent kinase 2), *CCNB1* (cyclin B1) [36], and *MKI67* [37], and with two slow-cycling genes, *CDKN1A* (cyclin-dependent kinase inhibitor 1A) and *G0S2* (G0/G1 switch gene 2) [38]. Our analysis revealed a negative correlation between *Cosmc* and *MKI67*, with no significant association for the other fast-cycling markers. In contrast, *Cosmc* positively correlated with the two genes associated with slow-cycling genes (Figure 3D). We also evaluated the association between cycling patterns and *Cosmc* expression in the Rembrandt and Gravendeel cohorts, but no similar profiles were observed compared to the TCGA dataset (Appendix A, Figure A2D). This discrepancy between cohorts may be attributed to heterogeneity of CSC subclones among cohorts [39] and the small fraction of slow-cycling clones within CSCs. Since slow-cycling clones represent only a small fraction of CSC subclones, their contribution may be under-represented in the datasets [40]. Additionally, CD44^+ CSCs are known to exhibit plasticity in their cycling behavior, which may further contribute to these differences [41].

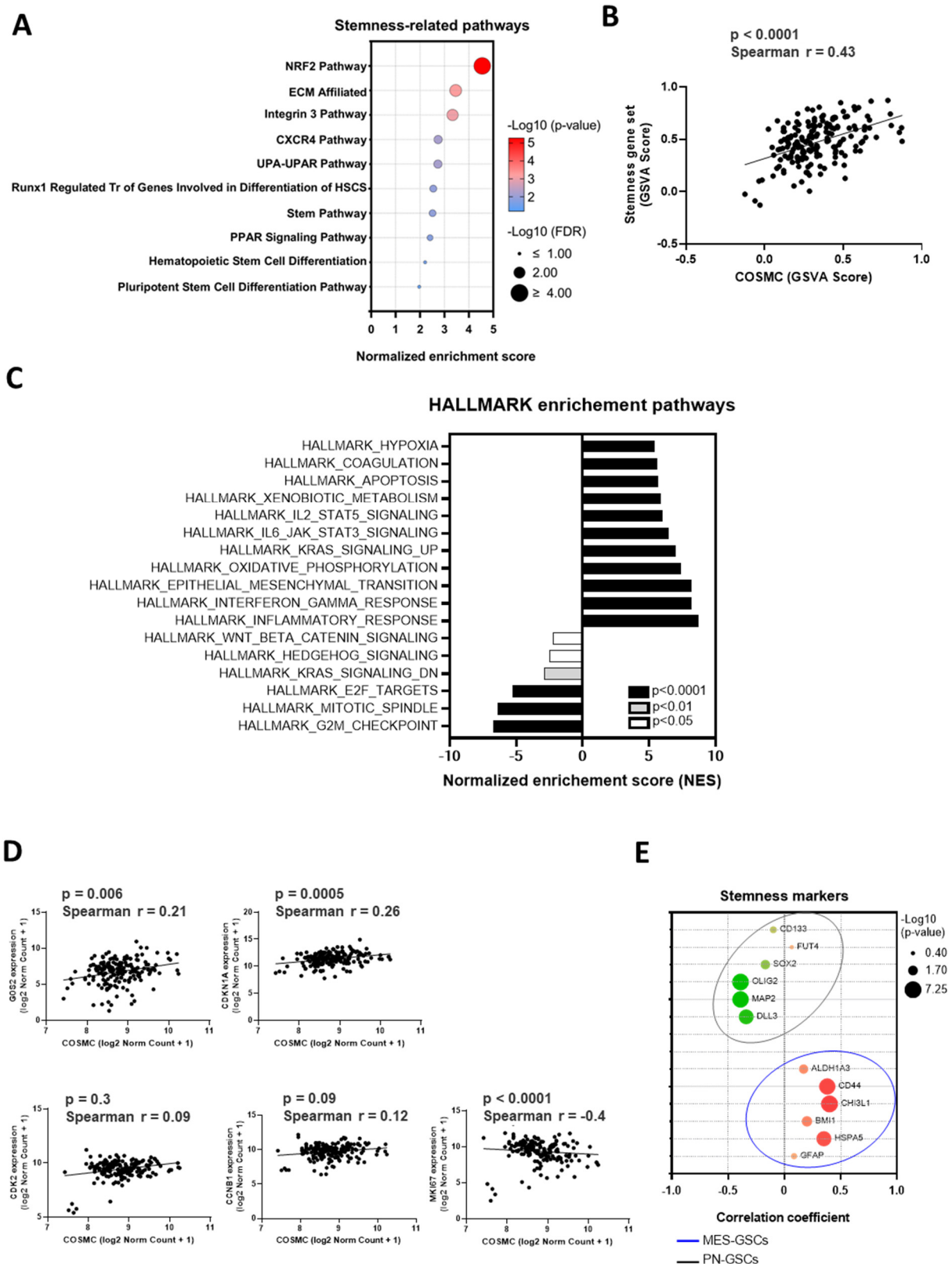


Figure 3. COSMC is associated with mesenchymal stem-like phenotype. (A) Top 10 stemness-related pathways from GSEA analysis enriched in the Cosmc group. Blue and red indicate the significance $-\log_{10}(p\text{-value})$ for enrichments of the pathway. (B) Spearman correlation between GSVAs Cosmc and enrichment scores obtained from the stem cell marker sets. (C) Hallmark gene sets from GSEA analysis enriched in Cosmc. The upregulated and downregulated significant signatures

are represented in the normalized enrichment score (NES) with a p -value shown with the code color. (D) Spearman correlation between *Cosmc* gene expression slow-cycling genes (*G0S2* and *CDKN1A*) and fast-cycling genes (*CDK2*, *CCNB1*, and *MKI67*), carried out by plotting \log_2 normalized count (norm count + 1) for each marker. *CDK2* (cyclin-dependent kinase 2), *CCNB1* (cyclin B1), *CDKN1A* (cyclin-dependent kinase inhibitor 1A), *G0S2* (G0/G1 switch gene 2). (E) Spearman correlation bubble plot of PN-GSC (black) and MES-GSC (purple) markers associated with *Cosmc* expression. The significance shows the correlation coefficient with a $-\log_{10}$ p -value.

In GBM, two stem cell subtypes have been identified: proneural GBM stem cells (PN-GSCs) and mesenchymal GBM stem cells (MES-GSCs), each defined by unique molecular and phenotypic markers. PN-GSCs are characterized by the expression of *MAP2*, *DLL2*, *OLIG2*, *SOX2*, *FUT4*, and *CD133*, while MES-GSCs exhibit markers such as *CD44*, *CHI3L1*, *GFAP*, *HSPA5*, *BMI1*, and *ALDH1A3* [42]. Studies have further demonstrated that *PPARG* [33], *CXCR4* [43], and *uPAR* [31] are specifically expressed by mesenchymal stem cells. The enrichment and stemness correlation with these markers, as shown in Figure 3A,B, suggest a potential correlation between *Cosmc* and mesenchymal subtypes. To determine the stem cell subtype associated with *Cosmc*, we conducted a Spearman correlation analysis, which showed a strong correlation between *Cosmc* and MES-GSC-associated markers (Figure 3E). We also confirmed that *Cosmc* was mostly distributed in the MES subtypes, but not in PN, in both cohorts of Rembrandt and Graveendeel (Appendix A, Figure A2E). Collectively, these findings indicate that *Cosmc* is associated with a stemness phenotype, associated with mesenchymal-like characteristics in GBM.

2.4. *COSMC* Is Significantly Associated with an Inflammatory Immune Environment

Immune cell infiltration within the tumor microenvironment (TME) plays a critical role in promoting tumor growth and therapy resistance. We explored the relationship between *Cosmc* expression and immune infiltration in GBM by analyzing immune and ESTIMATE scores from the ESTIMATE method. Our analysis identified a positive association between *Cosmc* expression and both immune and ESTIMATE scores (Figure 4A). To further investigate immune-related pathways associated with *Cosmc*, we compared immune cell pathway enrichment between high and low *Cosmc*-expression groups, based on the Biocarta and Reactome pathways. In Biocarta, pathways enriched in high *Cosmc* expression included interactions between lymphoid and non-lymphoid cells, antigen presentation signaling, and pathways involving B cells, neutrophils, and T cells (Figure 4B). In Reactome, *Cosmc* was linked with a variety of inflammatory immune cells, such as CD4 Th1-Th2 cells, natural killer T (NKT) cells, B cells, dendritic cells (DCs), granulocytes, monocytes, and neutrophils (Figure 4B). To assess the immune landscape associated with *Cosmc*, we analyzed immune cell populations correlated with *Cosmc* expression. *Cosmc* showed a strong association with antigen-presenting cells, including plasmacytoid dendritic cells (pDCs), DCs, and macrophages, as well as myeloid lineage cells like monocytes and MDSCs (Figure 4C). Among CD4 T cell subsets, *Cosmc* correlated positively with Th1 and Th2 cells, but showed no association with Th17 cells. *Cosmc* also positively correlated with CD4 T-regs and MDSCs, both key players in creating an immunosuppressive microenvironment in GBM [44]. Although *Cosmc*-enriched pathways included CD8 T cells (Figure 4C), *Cosmc* itself showed no significant correlation with CD8 T cell populations. Regarding B cells, *Cosmc* was not significantly correlated. Among NK cell subsets, only NK bright cells were positively correlated, while cytotoxic NK dim cells showed no significant association. Among granulocytes, eosinophils and mast cells did not correlate significantly with *Cosmc*, though NKT cells exhibited a positive correlation, consistent with pathway-enrichment findings (Figure 4B).

Overall, these findings suggest that *Cosmc* is closely associated with inflammatory and immunosuppressive immune cells, underscoring its potential role in modulating the immune landscape of the GBM tumor microenvironment.

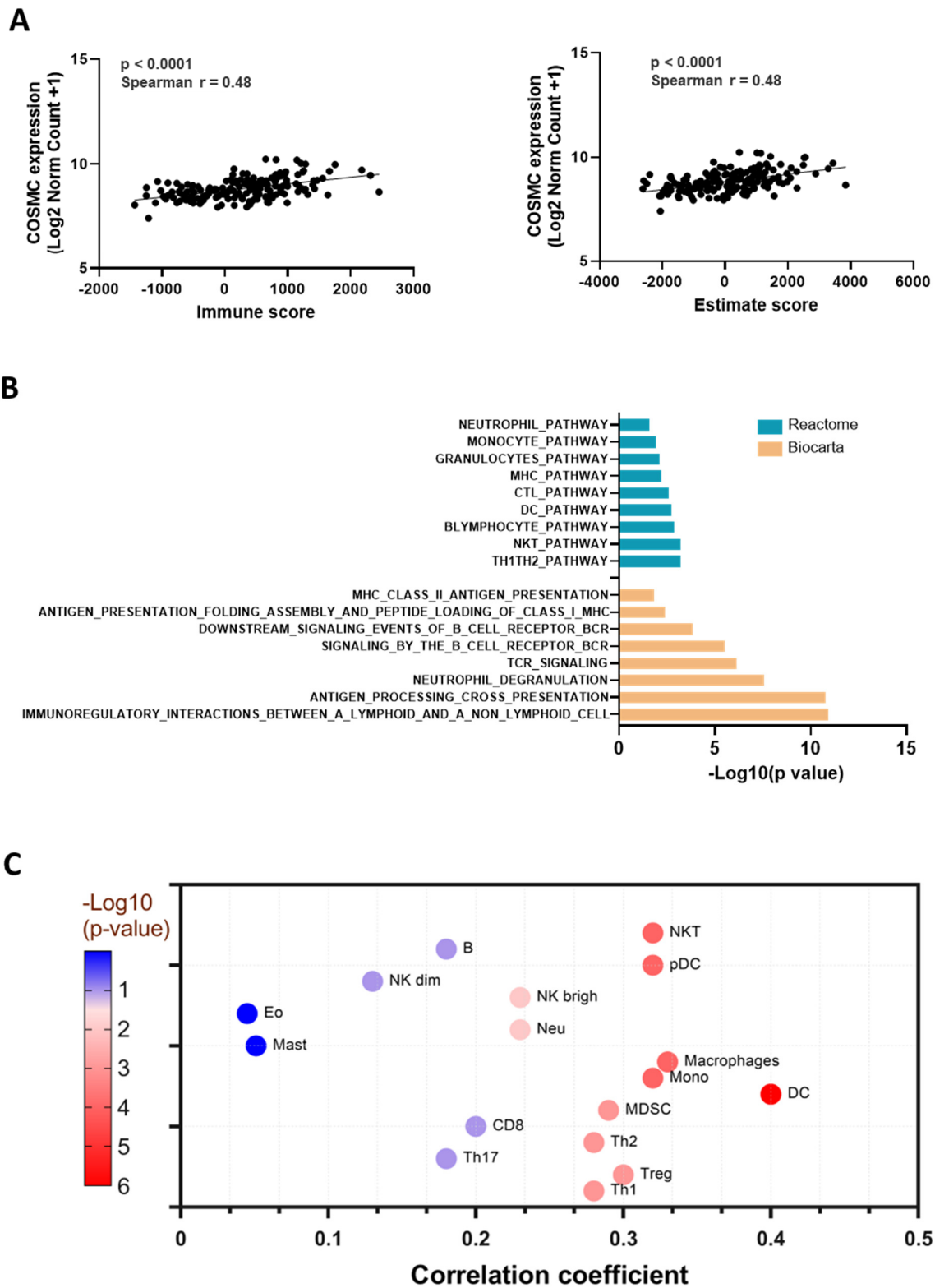


Figure 4. The association between COSMC and the immune microenvironment in GB. (A) Spearman correlation of immune and estimate score with *Cosmc* log2 (norm count + 1). (B) Top reactome and biocarta immune-related pathways for high *Cosmc* expression versus low expression. (C) Spearman correlation bubble plot of various immune cells associated with *Cosmc* gene expression. The significance shows the correlation coefficient with a $-\log_{10} p$ -value. Eo (eosinophils), Mast (mast cells), B (B cells), Neu (neutrophils), NKT (natural killer T cells), MDSC (myeloid-derived suppressor cells), Mono (monocytes), DC (dendritic cells).

2.5. COSMC Is Strongly Associated with Stroma Microenvironment

The stromal architecture plays a critical role in GBM tumor growth and sustainability. To assess Cosmc's relationship with stromal cells, we first analyzed its association with stroma using the ESTIMATE method, revealing a positive correlation between Cosmc expression and the stromal score (Figure 5A). We further examined specific stromal subsets within the GBM environment. Previous findings by Zarodniuk et al. showed that GBM can be categorized into two subtypes, based on extracellular matrix (ECM) enrichment, with high ECM levels correlating with poor immunotherapy response [45]. To explore this, we assessed ECM pathways enriched in Cosmc using GSEA, which identified several pathways, including integrin, collagen, proteoglycans, smooth muscle contraction, and adhesion molecules (Figure 5B). To deepen our understanding of ECM enrichment, we applied the ECM-high and ECM-low gene signatures defined by Zarodniuk et al., correlating these with Cosmc expression. Our analysis confirmed that Cosmc is negatively associated with ECM-low signatures but positively associated with high-ECM signatures (Figure 5C), suggesting that Cosmc is predominantly linked to a high-ECM environment. In the same study by Zarodniuk et al., high ECM was shown to enrich for pericytes, smooth muscle cells (SMCs), and perivascular fibroblasts (P-Fbs) with cancer-associated fibroblast (CAF) phenotypes, as well as endothelial cells, but not meningeal fibroblasts (M-Fbs). P-Fbs were particularly associated with poor responses to immune checkpoint inhibitors. Our correlation analysis indicated a strong association between Cosmc and CAFs, P-Fbs, and SMCs, while no significant correlation was observed with pericytes, endothelial cells, or M-Fbs (Figure 5C).

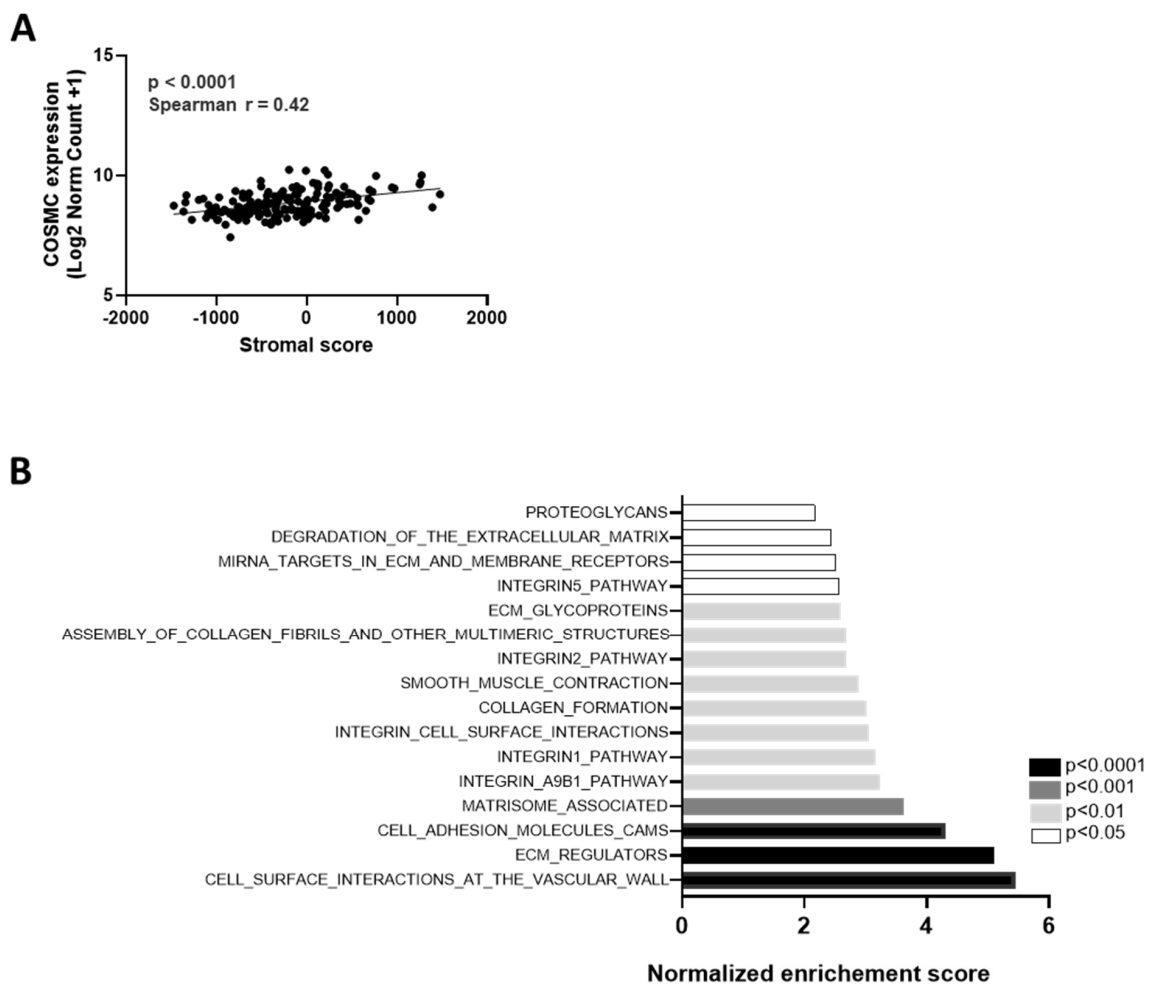


Figure 5. Cont.

C

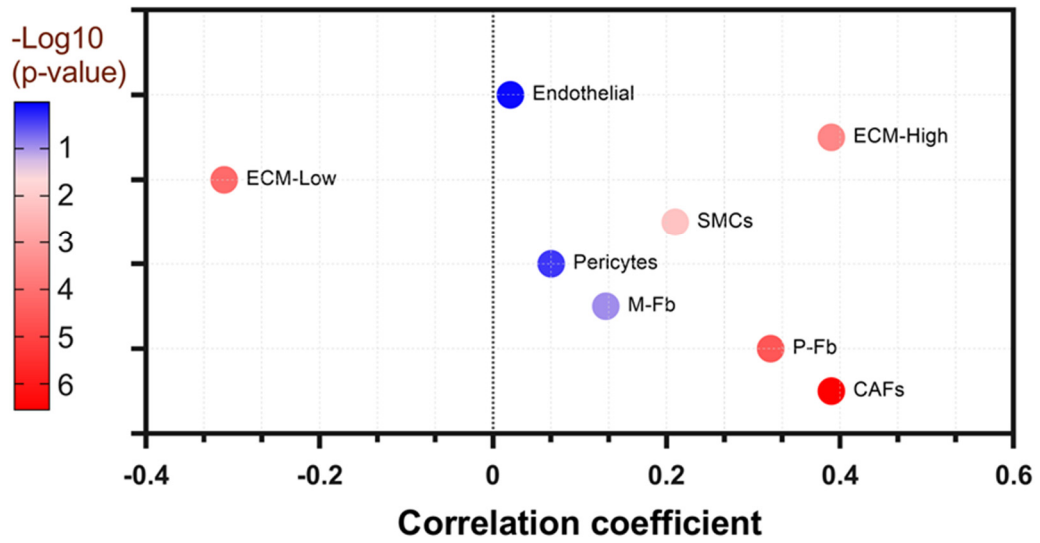


Figure 5. The association between COSMC with the stroma in GBM. (A) Spearman correlation test between stroma with Cosmc expression in GBM cohort. (B) The most significant canonical ECM signaling from GSEA for high Cosmc expression versus low expression, with a *p*-value shown with a code color. (C) Spearman correlation bubble plot of various stroma cells associated with Cosmc expression. CAFs—cancer-associated fibroblasts; P-Fb—perivascular fibroblasts, M-Fb—meningeal fibroblasts; SMCs—smooth muscle cells; ECM—extracellular matrix, high and low. The significance shows the correlation coefficient with a $-\log_{10}$ *p*-value.

Collectively, our findings suggest that Cosmc (Figure 6A) is linked to extensive ECM remodeling and a distinct distribution of stromal cell types (Figure 6B), highlighting its association with a high-ECM environment in GBM.

A

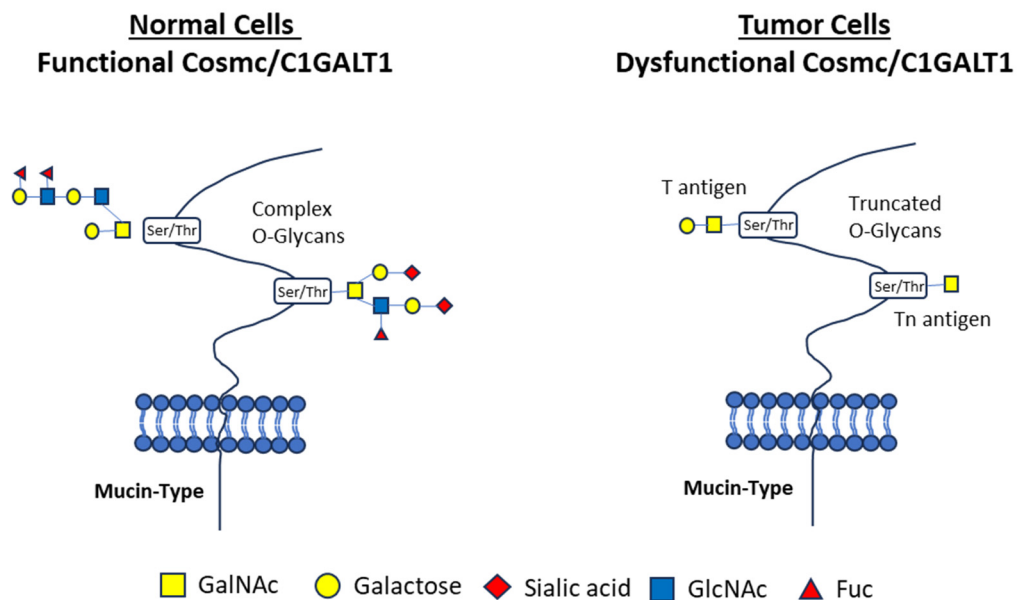


Figure 6. Cont.

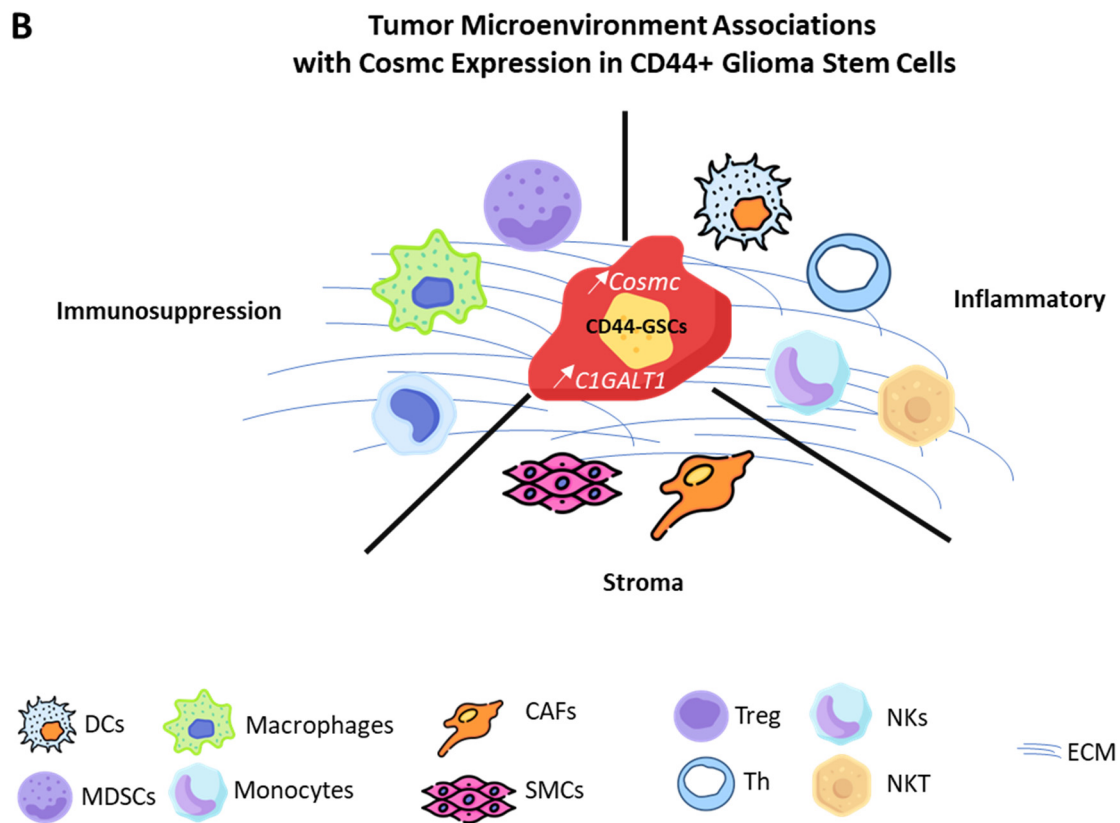


Figure 6. (A) Functional *Cosmc* in cells is essential for the proper production of complex O-glycans, which include various branched and elongated structures composed of N-acetylgalactosamine (GalNAc), galactose, sialic acid, N-acetylglucosamine (GlcNAc) and fucose (Fuc), and sometimes additional monosaccharides. These complex O-glycans play critical roles in the maintenance of cellular homeostasis. However, a dysfunctional *Cosmc*/*C1GALT1* leads to truncated O-glycans, such as the Tn and T antigen. The accumulation of these truncated O-glycans disrupts normal cellular functions and is associated with cancer progression, immune evasion, and poor clinical outcomes. (B) *Cosmc* expression was specifically elevated in CD44-positive glioblastoma stem cells (GSCs) and was associated with a more complex tumor microenvironment, characterized by the presence of inflammatory (DCs—dendritic cells, Th—T helper cells, NKs—natural killer cells, NKTs—natural killer T cells), immunosuppressive (MDSCs—myeloid-derived suppressor cells, Treg—T regulatory) and stromal cells (CAF—cancer-associated fibroblasts, SMC—smooth muscle cells). This elevated expression of *Cosmc* not only influenced the cellular composition of the TME, but also played a key role in modulating the extracellular matrix (ECM) architecture. By affecting ECM remodeling, *Cosmc* might influence cell adhesion, migration, and invasion, which are critical processes in GBM progression and therapeutic resistance.

3. Discussion

In this present study, we investigated the potential of O-glycosylation in differentiating CD133 and CD44 in GBM. The analysis of the GBM-TCGA dataset highlighted O-linked glycosylation pathways, highlighting the chaperone molecule *Cosmc*. Among the gene set of O-linked glycosylation of mucins, *Cosmc* stands out as a marker associated with aggressive features such as poor prognosis, stemness and mesenchymal stem cell-like phenotype. *Cosmc* expression was further associated with immune-related and extracellular matrix pathways, suggesting its potential as a biomarker for GSC subtypes and a target for new GBM therapies.

Cosmc (Core-1 β 1,3-galactosyltransferase-specific molecular chaperone) is an essential chaperone protein that facilitates the proper folding and functioning of the C1GALT1 (core 1 β 3-galactosyltransferase or T-synthase enzyme), which is crucial for O-glycan synthesis [26]. O-glycans are carbohydrate structures added to proteins, particularly mucin-type proteins, affecting their stability, signaling, and recognition by other cellular molecules [46,47].

In the context of cancer, alterations in O-glycosylation patterns are often observed and are known to influence tumor cell behavior, impacting cell proliferation, migration, adhesion, and immune evasion [48]. Cosmc dysfunction has been implicated in multiple cancer types, due to its critical role in maintaining proper glycosylation [25]. When Cosmc is defective or its expression is downregulated, similar to C1GALT1 [49], it results in defect O-glycans motifs, including the exposure of Tn (Figure 6A), and sialyl-Tn antigens (STn), well-known cancer-associated carbohydrate antigens [50]. These antigens, highly expressed at the surface of cells, make them interesting for histological and phenotypic target detection of cell changes in cancer [51]. In GBM, the Tn antigen has been found overexpressed in tumor tissue compared to normal samples [19]. Guan et al. found that Jacalin, a lectin that binds T antigen, was associated with progression-free survival, and reflects the corresponding levels of GBM tissues in the serum, making a potential non-invasive biomarker for GBM detection [52]. Moreover, its aberrant expression can promote cancer progression by altering cellular adhesion, affecting the tumor microenvironment, and potentially leading to immune escape. For instance, in carcinoma, Tn antigen expression is associated with immune inflammatory response, tumor differentiation and invasion [53]. These studies suggested that both immature and mature forms of T antigen modulated through Cosmc expression can be potentially relevant biomarkers in cancer.

Many studies have shown a significant association between Cosmc expression and cancer cell proliferation and tumorigenesis. For instance, Cosmc deletion in pancreatic cancer decreased proliferation, along with apoptosis, while enhancing migratory behavior, emphasizing the critical role of Cosmc in pancreatic cancer progression [54]. In breast cancer, Cosmc deficiency impaired tumor growth by disrupting CD44 expression and downstream MAPK signaling pathways. This effect was reversed upon restoring CD44, indicating the importance of its O-glycosylated form in maintaining CD44 stability and functionality [55]. Our analysis showed a positive correlation between Cosmc and CD44 expression in GBM, where Cosmc-enriched groups exhibited downregulation of proliferation-related pathways. In colon cancer, Cosmc overexpression promoted invasion and migration through EMT pathway activation, though independently of aberrant O-glycan accumulation [56]. Meanwhile, Cosmc loss, leading to truncated O-glycans, has been associated with increased invasion, metastasis, and stemness, through upregulation of CD133, CD44, and EMT-related mesenchymal markers, particularly in pancreatic cancer [57]. These findings illustrate the versatile role of O-glycosylation and Cosmc across cancer types. In this present study, we observed elevated Cosmc gene expression in GBM compared to normal brain tissue, along with enrichment in EMT and mesenchymal stem cell markers, with a stronger association with CD44 than CD133. However, experimental validation will be needed to clarify how Cosmc modulation in GSCs may influence CD133 and CD44 expression and related stemness properties.

The immune system often detects aberrant glycosylation patterns as non-self, potentially triggering immune surveillance and an anti-tumor response [58,59]. For instance, blocking Tn antigen maturation through genetic modification of Cosmc increases the susceptibility of breast and pancreatic cancer cells to antibody-dependent cellular cytotoxicity (ADCC) mediated by NK cells and cytotoxic CD8 T lymphocytes (CTLs) [60]. In GBM, NK cells play a dual role. High infiltration of cytotoxic NK cells within GBM tumor tissue can selectively target undifferentiated GSCs expressing elevated CD44, in contrast to cells with low CD44 expression and more differentiated phenotypes [61]. Simultaneously, NK cells promote GSC differentiation through the release of IFN γ and TNF α , leading to resistance against NK cell-mediated cytotoxicity [62]. Our data reveal a significant correlation with NK bright cells; NK subsets with low cytotoxicity but high cytokine production,

including IFN γ and TNF α [63]. This suggests that NK bright cells, rather than NK dim cells, may maintain GSC stemness by secreting IFN γ , supporting immune evasion and tumor persistence.

However, in some cases, altered glycosylation can actively promote immune evasion [64]. Cornelissen et al. demonstrated that CRISPR/Cas9 knockout of *Cosmc* in colorectal cancer cells, leading to increased Tn antigen expression, resulted in reduced cytotoxic CD8+ T cells and an increased presence of immunosuppressive cells, such as MDSCs. This alteration also enriched pathways related to antigen processing and presentation [65]. Additionally, *Cosmc* loss impacts myeloid cell function, as macrophage galactose-type lectins (MGLs) expressed by DCs and macrophages bind to Tn antigen. In lung cancer, *Cosmc* deletion led to Tn antigen upregulation, reprogramming DCs into more tolerogenic states that promote pro-tumoral cytokine release and immunosuppression [66]. In GBM, overexpression of Tn antigen similarly correlated with an increase in immunosuppressive macrophages, both in vivo and in patient tissue samples [19]. Our findings reveal that *Cosmc* is associated with immunosuppressive features, showing a strong correlation with MDSCs, macrophages, and DCs, which likely suggests an immunosuppressive microenvironment in GBM.

The TME in GBM also includes stromal cells that contribute to immunosuppressive functions. Zarodniuk et al. demonstrated that perivascular fibroblasts in the GBM stroma are associated with poor prognosis and resistance to immunotherapy, as they facilitate the recruitment of tumor-associated macrophages (TAMs) and enhance stemness properties in cancer cells [45]. Their study also identified distinct ECM profiles, classifying GBM into high- and low-ECM subtypes, with the high-ECM subtype correlating with poorer outcomes. In GBM, ECM remodeling is crucial for tumor progression, reshaping the structural and biochemical landscape to promote cancer cell migration, invasion, and survival [67]. Additionally, Madzharova et al. found that *Cosmc* inactivation in breast cell lines led to an increase in Tn antigen, which heightened ECM susceptibility to MMP9-mediated proteolysis [68]. Collectively, these findings suggest that *Cosmc* may serve as a biomarker of aggressiveness, and is supported by our analysis, which shows that an enrichment of ECM signatures positively correlated with perivascular fibroblast presence.

To provide a balanced perspective, it is essential to highlight the limitations of a bioinformatic approach. (i) First, while we utilized the public and comprehensive TCGA-GBM database, the predictive association between *Cosmc* and GBM is primarily derived from publicly available datasets. These datasets may inherently carry biases and discrepancies, due to variations in sample collection, processing methodologies, cohort demographics, and GBM molecular and cellular heterogeneity. (ii) Additionally, although CD44 and CD133 are often used as GSC markers, they may not exclusively reflect stem cells, since these markers can also be expressed by non-GSC populations. (iii) Third, although bioinformatic analyses provide valuable initial insights for hypothesis generation and can reduce the cost and time required for research, experimental validation remains crucial. Establishing the association between *Cosmc* and GSCs will require techniques such as knockout KO systems, proteomics, metabolomics, and spatial transcriptomics to verify correlations and understand the role of *Cosmc* in GBM tumorigenesis. Employing multimodal approaches that integrate diverse data types, including biomedical and clinical information, will enhance our understanding of the clinical relevance of *Cosmc* as a biomarker [69].

Collectively, our bioinformatic findings showed the potential role of *Cosmc* in GBM, particularly in differentiating CD44- and CD133-associated stem cell-like populations. *Cosmc* emerges as a promising biomarker associated with mesenchymal phenotype, stemness characteristics, and a more aggressive tumor microenvironment in GBM. Although the bioinformatic methods have evolved as an important tool to accelerate precision oncology, further experimental validation will be essential to translate the in silico findings on *Cosmc* into actionable insights for GBM research and treatment.

4. Methods

4.1. Data Collection

We downloaded the transcriptome data of the Ivy GBM atlas project (Ivy-GAP) (n = 270), the Repository of Molecular Brain Neoplasia Data (REMBRANDT) (normal brain n = 28, GBM n = 219) and Gravendeel dataset (normal brain n = 8, GBM n = 159) from Gliovis [70]. The datasets GSE85297, GSE34152 and GSE77530 were downloaded from GEO Omnibus. The GSE85297 dataset represents RNA-sequencing of primary GBM cultured into tumorspheres and subsequently sorted into CD133⁻ and CD133⁺ cell populations [71]. The GSE34152 dataset contains microarray data from two GBM samples, sorted based on the CD133 marker [72]. The GSE77530 dataset comprises RNA sequencing data from 32 GBM patients [73].

4.2. Molecular, Clinical and Tumor Environment Analysis Based on Xena Analysis

The UCSC Xena database [74] is an online tool for visualizing and analyzing multi-omic and clinical/phenotype data from publicly accessible datasets. Xena was employed to perform gene set enrichment analysis (GSEA) to identify O-glycosylation signatures in CD44 and high-CD133 groups. The differently expressed pathways with $\text{adj-}p < 0.05$ and differential multiplicity $\text{Log}_2\text{FC} > 1$ were considered significant. We further categorize the key O-glycosylation gene from the O-linked_glycosylation_of_Mucins sets between CD44 and CD133, using a Venn diagram.

The TCGA-GBM cohort (n = 172) from UCSC Xena was downloaded and utilized to extract overall survival and progression-free interval, and were plotted as forest plots or in Kaplan–Meier curves. In addition, the O-glycosylation gene core, and the slow- and fast-cycling gene expression levels were also extracted.

Additionally, Xena was employed to perform gene set enrichment analysis (GSEA) to compare stemness-related pathways, the hallmark and canonical pathways between Cosmc high (n = 86) and low groups (n = 86), using the median expression as cutoff. The differently expressed pathways with $\text{adj-}p < 0.05$ and differential multiplicity $\text{Log}_2\text{FC} > 1$ were considered significant.

To assess the correlation between Cosmc expression and PN-GSCs and MES-GSCs phenotypes, we utilized gene sets from Wang et al., and analyzed the relationship between Cosmc expression and these specific gene sets. PN-GSCs are defined by *MAP2* (Microtubule-Associated Protein 2), *DLL2* (Delta-Like Ligand 2), *OLIG2* (Oligodendrocyte Transcription Factor 2), *SOX2* (SRY-Box Transcription Factor 2), *FUT4* (Fucosyltransferase 4), and *CD133* (Prominin-1), while MES-GSCs are defined by the expression of *CD44* (CD44 Antigen), *CHI3L1* (Chitinase-3-Like Protein 1), *GFAP* (Glial Fibrillary Acidic Protein), *HSPA5* (Heat Shock Protein Family A (Hsp70) Member 5), *BMI1* (BMI1 Proto-Oncogene, Polycomb Ring Finger), and *ALDH1A3* (Aldehyde Dehydrogenase 1 Family Member A3) [42].

For immune distribution, we used the “correlation analysis” module in GEPIA to compare the Cosmc gene with immune gene signatures, extracting the correlation coefficients and *p*-values. The results were then visualized in a heatmap to display the relationships between gene set signatures and immune cell infiltration.

4.3. Gene Expression Based on GEPIA Analysis

GEPIA [75] is an online tool that provides gene expression, state/grade, correlation, and survival data based on the TCGA and normal Genotype-Tissue Expression (GTEx) projects. Normalized gene expression was measured as transcripts per kilobase million (TPM) values. The $\text{log}_2 \text{TPM} + 1$ expression levels of the 14 genes including Cosmc (6 genes enriched in the CD44 group and 8 genes from CD133 from the O-linked_glycosylation_of_Mucins gene set) were compared between GBM and corresponding normal brain tissues from the GTEx database. The gene expression of C1GALT1, ST3GAL1 and B3NGT3 comparing matched normal brain tissue to GBM was also extracted from the GEPIA database. Stroma cell gene sets were taken from various studies, and the correlation between the gene sets, and Cosmc expression, was assessed using the corre-

lation analysis from Gepia. To identify ECM cell enrichment, we used the expression of gene sets from Zarodniuk M et al. and evaluated the correlation between Cosmc with the gene sets, based on GEPIA. The stroma cells included perivascular fibroblasts (P-Fb-*FBLN1*, *LAMA2*), meningeal fibroblasts (M-Fb-*SLC4A4*, *KCNMA1*), pericytes (*PDGFRB*, *COL4A1*), smooth muscle cells (SMC; *ACTA2*), ECM low (*CDK5R1*, *BRSK2*), and ECM high (*COL5A2*, *COL1A2*, *COL3A1*, *COL1A1*, *COL6A3*, *COL5A1*, *COL6A2*, *COL8A1*, *LAMB1*, *LAMC1*, *POSTN*, *FN1*) [45]. Cancer-associated fibroblasts were identified based on the expression of six genes (CAFs-*ACTA2*, *FAP*, *PDPN*, *DES*, *THY1*, and *S100A4*) from Jain et al. [76]. The endothelial signature was identified using the Cell Marker 2.0 with the following genes: *CLDN5*, *FLT1*, *A2M*, *APOLD1*, and *TM4SF1* [77].

4.4. Estimate Scores

The ESTIMATE platform [78] was used for extracting the immune score, stromal score, and ESTIMATE score of each TCGA sample ($n = 166$), and the correlation between GBM samples and corresponding Cosmc gene expression from Xena was evaluated.

4.5. GSVA Score for Stemness Correlation

A Gene Set Variation Analysis (GSVA) score for a Cosmc and the stem cell gene sets (*NRF2*, *Integrin3-ITGAV*, *CXCR4*, *uPA*, *uPAR*, *RUNX1* and *PPARG*) were extracted to analyze the correlation between Cosmc and stemness. GSVA is an unsupervised gene set-enrichment method that calculates enrichment scores for predefined gene sets, representing various biological processes in individual samples [79]. GSVA scores for each signature were generated using the Gene Set Cancer Analysis GCVAlite webtool [80], and Spearman correlation was plotted.

Author Contributions: S.S.A. corrected, revised, provided critical feedback, contributed ideas, and finalized the manuscript. R.A. conceived the original idea, wrote, revised, and supplemented the manuscript. All authors have read and agreed to the published version of the manuscript.

Funding: This research received no external funding.

Institutional Review Board Statement: Not applicable.

Informed Consent Statement: Not applicable.

Data Availability Statement: The data presented in this study are available upon request from the corresponding author.

Conflicts of Interest: The authors declare no conflicts of interest.

Appendix A

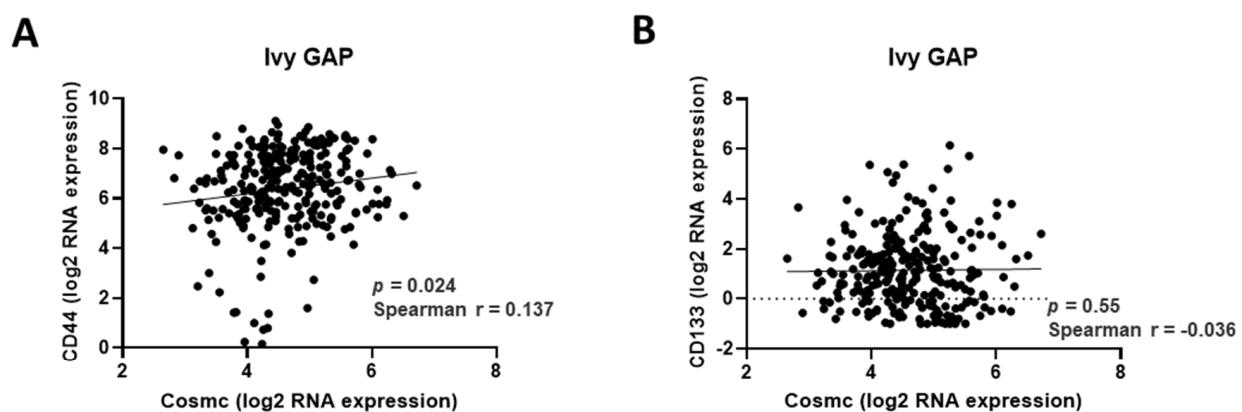


Figure A1. Cont.

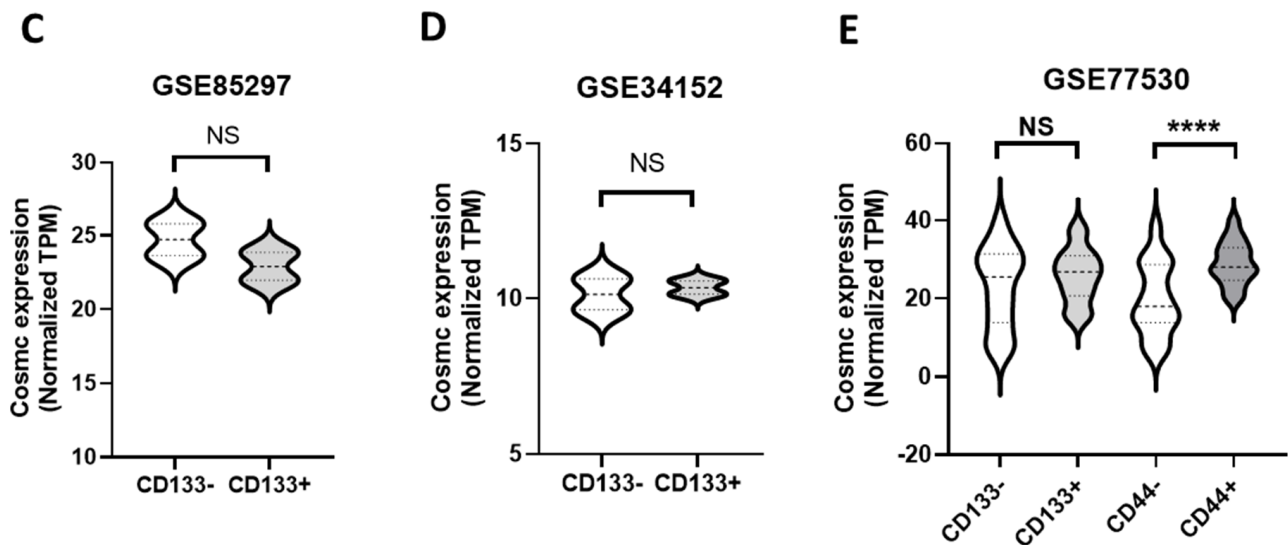


Figure A1. Cosmc is strongly associated with CD44 across several GBM datasets. (A) Spearman correlation between normalized log₂ gene expression of CD44 and Cosmc in the Ivy Glioblastoma Atlas Project (Ivy-GAP). (B) Spearman correlation between normalized log₂ gene expression of CD133 and Cosmc in the Ivy Glioblastoma Atlas Project (Ivy-GAP). Statistical significance is indicated by the *p*-value. (C) Cosmc gene expression assessed in CD133⁻ and CD133⁺ CSCs sorted using CD133 markers from the GSE85297 dataset. The expression is displayed in transformed normalized transcript per millions (TPM). (D) Cosmc gene expression assessed in CD133⁻ and CD133⁺ GBM samples, sorted using CD133 markers from the GSE34152 dataset. (E) Cosmc gene expression analyzed in CD133⁻/CD133⁺ and CD44⁻/CD44⁺ GBM groups, stratified based on the median gene expression levels of CD133 and CD44 in the GSE77530 dataset. Statistical analysis comparing the two groups was performed using an unpaired Student's *t*-test. **** *p* < 0.0001, NS—non significant.

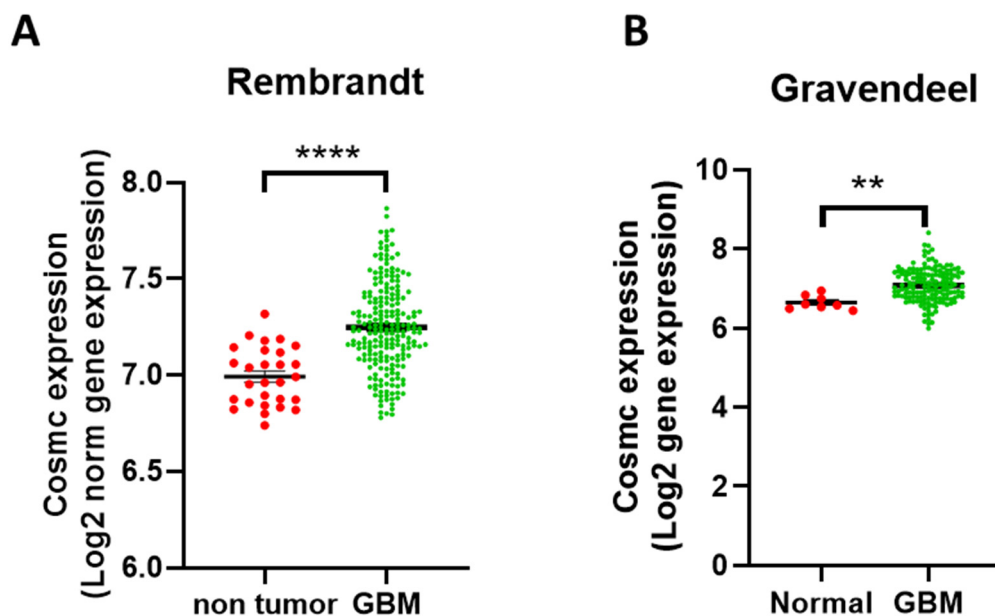


Figure A2. Cont.

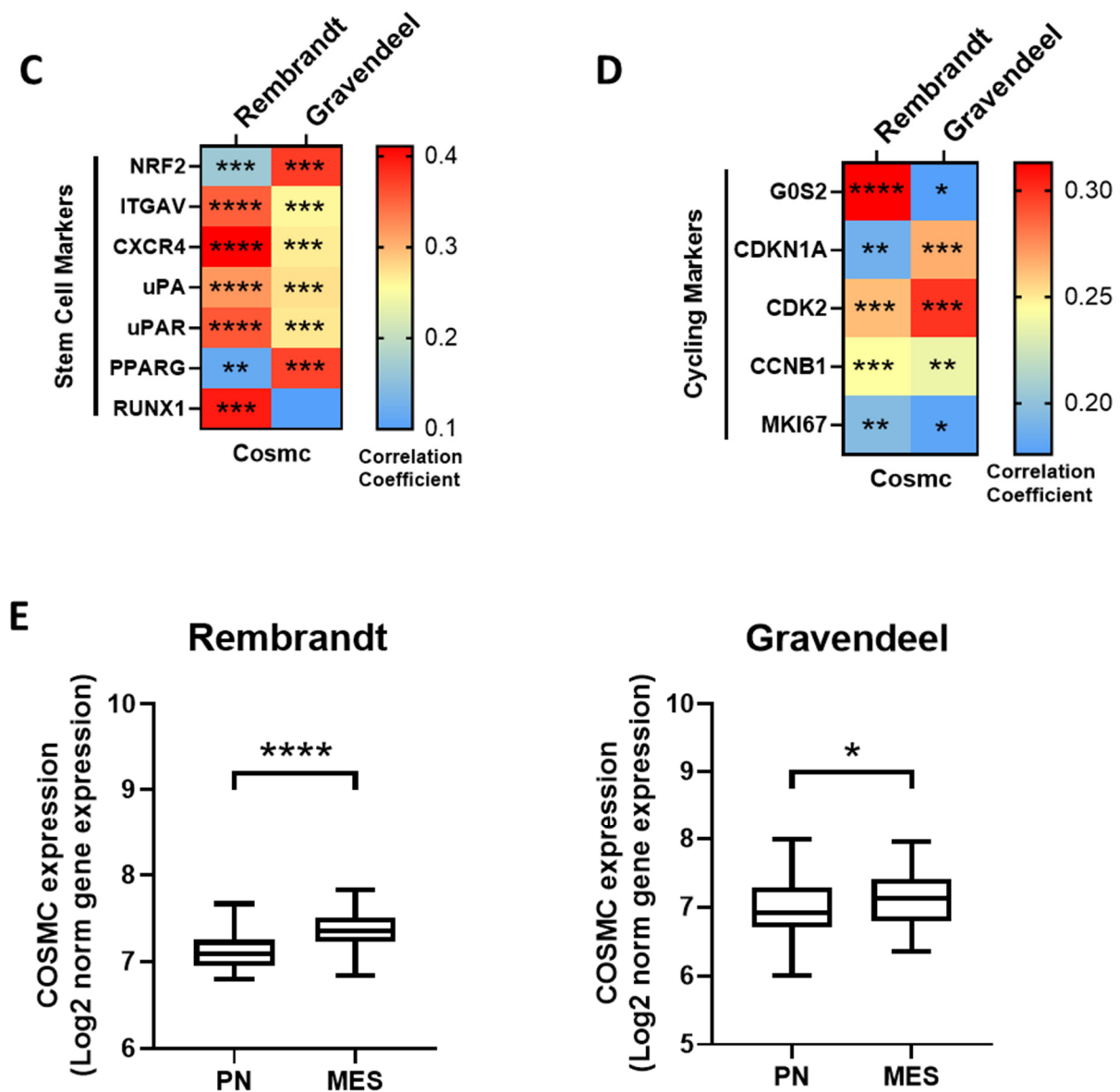


Figure A2. Cosmc is enriched in stemness and mesenchymal-like phenotype across different GBM datasets. (A) Differential Cosmc gene expression comparing normal brain tissue (red) to GBM samples (green) in the Rembrandt cohort, using unpaired Student's *t*-tests (**** $p < 0.001$). (B) Differential Cosmc gene expression comparing normal brain tissue (red) to GBM samples (green) in the Gravendeel cohort, using unpaired Student's *t*-tests (** $p < 0.01$). (C) Heatmap displaying the Spearman correlation between the Cosmc with GBM stem cell markers (*NRF2*, *ITGA*, *CXCR4*, *uPA*, *uPAR*, *PPARG* and *RUNX1*) in the Rembrandt and Gravendeel cohorts. A statistical test was performed with the Spearman correlation test, and the significant *p* value is displayed on the heatmap. **** $p < 0.0001$, *** $p < 0.001$, ** $p < 0.01$. (D) Heatmap displaying the Spearman correlation between the Cosmc with GBM slow-cycling genes (*G0S2* and *CDKN1A*) and with fast-cycling genes (*CDK2*, *CCNB1*, and *MKI67*) in the Rembrandt and Gravendeel cohorts. A statistical test was performed with the Spearman correlation test, and the significant *p* value is displayed on the heatmap. **** $p < 0.0001$, *** $p < 0.001$, ** $p < 0.01$, * $p < 0.05$. (E) Cosmc gene expression in proneural (PN) and mesenchymal (MES) subtypes in Rembrandt and Gravendeel cohorts. Statistical analysis comparing the two groups was performed using an unpaired Student's *t*-test. **** $p < 0.0001$, * $p < 0.05$.

References

1. Noch, E.K.; Ramakrishna, R.; Magge, R. Challenges in the treatment of glioblastoma: Multisystem mechanisms of therapeutic resistance. *World Neurosurg.* **2018**, *116*, 505–517. [[CrossRef](#)] [[PubMed](#)]
2. Alves, A.L.V.; Gomes, I.N.F.; Carloni, A.C.; Rosa, M.N.; da Silva, L.S.; Evangelista, A.F.; Reis, R.M.; Silva, V.A.O. Role of glioblastoma stem cells in cancer therapeutic resistance: A perspective on antineoplastic agents from natural sources and chemical derivatives. *Stem Cell Res. Ther.* **2021**, *12*, 206. [[CrossRef](#)] [[PubMed](#)]
3. Chiariello, M.; Inzalaco, G.; Barone, V.; Gherardini, L. Overcoming challenges in glioblastoma treatment: Targeting infiltrating cancer cells and harnessing the tumor microenvironment. *Front. Cell. Neurosci.* **2023**, *17*, 1327621. [[CrossRef](#)] [[PubMed](#)]
4. Gimple, R.C.; Bhargava, S.; Dixit, D.; Rich, J.N. Glioblastoma stem cells: Lessons from the tumor hierarchy in a lethal cancer. *Genes Dev.* **2019**, *33*, 591–609. [[CrossRef](#)]
5. Liu, Q.; Nguyen, D.H.; Dong, Q.; Shitaku, P.; Chung, K.; Liu, O.Y.; Tso, J.L.; Liu, J.Y.; Konkankit, V.; Cloughesy, T.F.; et al. Molecular properties of CD133+ glioblastoma stem cells derived from treatment-refractory recurrent brain tumors. *J. Neurooncol* **2009**, *94*, 1–19. [[CrossRef](#)]
6. Abdoli Shadbad, M.; Nejadi Orang, F.; Baradaran, B. CD133 significance in glioblastoma development: In silico and in vitro study. *Eur. J. Med. Res.* **2024**, *29*, 154. [[CrossRef](#)]
7. Inoue, A.; Ohnishi, T.; Nishikawa, M.; Ohtsuka, Y.; Kusakabe, K.; Yano, H.; Tanaka, J.; Kunieda, T. A narrative review on cd44's role in glioblastoma invasion, proliferation, and tumor recurrence. *Cancers* **2023**, *15*, 4898. [[CrossRef](#)]
8. Hassn Mesrati, M.; Behrooz, A.B.; Y Abuhamad, A.; Syahir, A. Understanding Glioblastoma Biomarkers: Knocking a Mountain with a Hammer. *Cells* **2020**, *9*, 1236. [[CrossRef](#)]
9. Brown, D.V.; Filiz, G.; Daniel, P.M.; Hollande, F.; Dworkin, S.; Amiridis, S.; Kountouri, N.; Ng, W.; Morokoff, A.P.; Mantamadiotis, T. Expression of CD133 and CD44 in glioblastoma stem cells correlates with cell proliferation, phenotype stability and intra-tumor heterogeneity. *PLoS ONE* **2017**, *12*, e0172791. [[CrossRef](#)]
10. Beier, D.; Hau, P.; Proescholdt, M.; Lohmeier, A.; Wischhusen, J.; Oefner, P.J.; Aigner, L.; Brawanski, A.; Bogdahn, U.; Beier, C.P. CD133(+) and CD133(-) glioblastoma-derived cancer stem cells show differential growth characteristics and molecular profiles. *Cancer Res.* **2007**, *67*, 4010–4015. [[CrossRef](#)]
11. Silver, A.; Feier, D.; Ghosh, T.; Rahman, M.; Huang, J.; Sarkisian, M.R.; Deleyrolle, L.P. Heterogeneity of glioblastoma stem cells in the context of the immune microenvironment and geospatial organization. *Front. Oncol.* **2022**, *12*, 1022716. [[CrossRef](#)] [[PubMed](#)]
12. Khan, I.; Mahfooz, S.; Karacam, B.; Elbasan, E.B.; Akdur, K.; Karimi, H.; Sakarcan, A.; Hatiboglu, M.A. Glioma cancer stem cells modulating the local tumor immune environment. *Front. Mol. Neurosci.* **2022**, *15*, 1029657. [[CrossRef](#)] [[PubMed](#)]
13. White, J.; White, M.P.J.; Wickremesekera, A.; Peng, L.; Gray, C. The tumour microenvironment, treatment resistance and recurrence in glioblastoma. *J. Transl. Med.* **2024**, *22*, 540. [[CrossRef](#)]
14. Amin, R.; Mourcin, F.; Uhel, F.; Pangault, C.; Ruminy, P.; Dupré, L.; Guirricc, M.; Marchand, T.; Fest, T.; Lamy, T.; et al. DC-SIGN-expressing macrophages trigger activation of mannoseylated IgM B-cell receptor in follicular lymphoma. *Blood* **2015**, *126*, 1911–1920. [[CrossRef](#)]
15. Khan, T.; Cabral, H. Abnormal glycosylation of cancer stem cells and targeting strategies. *Front. Oncol.* **2021**, *11*, 649338. [[CrossRef](#)]
16. Wang, C.; Xiong, K. Glycosylation modification identifies novel molecular phenotypes and prognostic stratifications of glioma. *Gene* **2022**, *836*, 146677. [[CrossRef](#)]
17. Tokumura, K.; Sadamori, K.; Yoshimoto, M.; Tomizawa, A.; Tanaka, Y.; Fukasawa, K.; Hinoi, E. The Bioinformatics Identification of Potential Protein Glycosylation Genes Associated with a Glioma Stem Cell Signature. *BioMedInformatics* **2024**, *4*, 75–88. [[CrossRef](#)]
18. Radhakrishnan, P.; Dabelsteen, S.; Madsen, F.B.; Francavilla, C.; Kopp, K.L.; Steentoft, C.; Vakhrushev, S.Y.; Olsen, J.V.; Hansen, L.; Bennett, E.P.; et al. Immature truncated O-glycophenotype of cancer directly induces oncogenic features. *Proc. Natl. Acad. Sci. USA* **2014**, *111*, E4066–75. [[CrossRef](#)]
19. Dusoswa, S.A.; Verhoeff, J.; Abels, E.; Méndez-Huergo, S.P.; Croci, D.O.; Kuijper, L.H.; de Miguel, E.; Wouters, V.M.C.J.; Best, M.G.; Rodriguez, E.; et al. Glioblastomas exploit truncated O-linked glycans for local and distant immune modulation via the macrophage galactose-type lectin. *Proc. Natl. Acad. Sci. USA* **2020**, *117*, 3693–3703. [[CrossRef](#)]
20. Sun, Y.-F.; Zhang, L.-C.; Niu, R.-Z.; Chen, L.; Xia, Q.-J.; Xiong, L.-L.; Wang, T.-H. Predictive potentials of glycosylation-related genes in glioma prognosis and their correlation with immune infiltration. *Sci. Rep.* **2024**, *14*, 4478. [[CrossRef](#)]
21. Aghamiri, S.S.; Amin, R. Cancer stem cell metastatic checkpoints and glycosylation patterns: Implications for therapeutic strategies. *Kinases Phosphatases* **2024**, *2*, 151–165. [[CrossRef](#)]
22. Gao, T.; Wen, T.; Ge, Y.; Liu, J.; Yang, L.; Jiang, Y.; Dong, X.; Liu, H.; Yao, J.; An, G. Disruption of Core 1-mediated O-glycosylation oppositely regulates CD44 expression in human colon cancer cells and tumor-derived exosomes. *Biochem. Biophys. Res. Commun.* **2020**, *521*, 514–520. [[CrossRef](#)] [[PubMed](#)]
23. Leon, F.; Seshacharyulu, P.; Nimmakayala, R.K.; Chugh, S.; Karmakar, S.; Nallasamy, P.; Vengoji, R.; Rachagani, S.; Cox, J.L.; Mallya, K.; et al. Reduction in O-glycome induces differentially glycosylated CD44 to promote stemness and metastasis in pancreatic cancer. *Oncogene* **2022**, *41*, 57–71. [[CrossRef](#)] [[PubMed](#)]
24. Liu, Y.; Chen, P.; Xu, L.; Wang, B.; Zhang, S.; Wang, X. GALNT2 sustains glioma stem cells by promoting CD44 expression. *Aging* **2023**, *15*, 2208–2220. [[CrossRef](#)] [[PubMed](#)]
25. Xiang, T.; Qiao, M.; Xie, J.; Li, Z.; Xie, H. Emerging roles of the unique molecular chaperone cosmc in the regulation of health and disease. *Biomolecules* **2022**, *12*, 1732. [[CrossRef](#)]

26. Wang, Y.; Ju, T.; Ding, X.; Xia, B.; Wang, W.; Xia, L.; He, M.; Cummings, R.D. Cosmc is an essential chaperone for correct protein O-glycosylation. *Proc. Natl. Acad. Sci. USA* **2010**, *107*, 9228–9233. [[CrossRef](#)]
27. Petrosyan, A. Onco-Golgi: Is Fragmentation a Gate to Cancer Progression? *Biochem. Mol. Biol. J.* **2015**, *1*, 16. [[CrossRef](#)]
28. Zhu, J.; Wang, H.; Ji, X.; Zhu, L.; Sun, Q.; Cong, Z.; Zhou, Y.; Liu, H.; Zhou, M. Differential Nrf2 expression between glioma stem cells and non-stem-like cells in glioblastoma. *Oncol. Lett.* **2014**, *7*, 693–698. [[CrossRef](#)]
29. Messé, M.; Bernhard, C.; Foppolo, S.; Thomas, L.; Marchand, P.; Herold-Mende, C.; Idbaih, A.; Kessler, H.; Etienne-Selloum, N.; Ochoa, C.; et al. Hypoxia-driven heterogeneous expression of $\alpha 5$ integrin in glioblastoma stem cells is linked to HIF-2 α . *Biochim. Biophys. Acta Mol. Basis Dis.* **2024**, *1870*, 167471. [[CrossRef](#)]
30. Ehtesham, M.; Mapara, K.Y.; Stevenson, C.B.; Thompson, R.C. CXCR4 mediates the proliferation of glioblastoma progenitor cells. *Cancer Lett.* **2009**, *274*, 305–312. [[CrossRef](#)]
31. Gilder, A.S.; Natali, L.; Van Dyk, D.M.; Zalfa, C.; Banki, M.A.; Pizzo, D.P.; Wang, H.; Klemke, R.L.; Mantuano, E.; Gonias, S.L. The urokinase receptor induces a mesenchymal gene expression signature in glioblastoma cells and promotes tumor cell survival in neurospheres. *Sci. Rep.* **2018**, *8*, 2982. [[CrossRef](#)] [[PubMed](#)]
32. Zhao, K.; Cui, X.; Wang, Q.; Fang, C.; Tan, Y.; Wang, Y.; Yi, K.; Yang, C.; You, H.; Shang, R.; et al. RUNX1 contributes to the mesenchymal subtype of glioblastoma in a TGF β pathway-dependent manner. *Cell Death Dis.* **2019**, *10*, 877. [[CrossRef](#)] [[PubMed](#)]
33. Gupta, G.; Singhvi, G.; Chellappan, D.K.; Sharma, S.; Mishra, A.; Dahiya, R.; de Jesus Andreoli Pinto, T.; Dua, K. Peroxisome proliferator-activated receptor gamma: Promising target in glioblastoma. *Panminerva Med.* **2018**, *60*, 109–116. [[CrossRef](#)] [[PubMed](#)]
34. Xie, X.P.; Laks, D.R.; Sun, D.; Ganbold, M.; Wang, Z.; Pedraza, A.M.; Bale, T.; Tabar, V.; Brennan, C.; Zhou, X.; et al. Quiescent human glioblastoma cancer stem cells drive tumor initiation, expansion, and recurrence following chemotherapy. *Dev. Cell* **2022**, *57*, 32–46.e8. [[CrossRef](#)]
35. Majc, B.; Sever, T.; Zarić, M.; Breznik, B.; Turk, B.; Lah, T.T. Epithelial-to-mesenchymal transition as the driver of changing carcinoma and glioblastoma microenvironment. *Biochim. Biophys. Acta Mol. Cell Res.* **2020**, *1867*, 118782. [[CrossRef](#)]
36. Min, M.; Spencer, S.L. Spontaneously slow-cycling subpopulations of human cells originate from activation of stress-response pathways. *PLoS Biol.* **2019**, *17*, e3000178. [[CrossRef](#)]
37. Man, K.-H.; Wu, Y.; Gao, Z.; Spreng, A.-S.; Keding, J.; Mangei, J.; Boskovic, P.; Mallm, J.-P.; Liu, H.-K.; Imbusch, C.D.; et al. SOX10 mediates glioblastoma cell-state plasticity. *EMBO Rep.* **2024**, *25*, 5113–5140. [[CrossRef](#)]
38. Aulestia, F.J.; Néant, I.; Dong, J.; Haiech, J.; Kilhoffer, M.-C.; Moreau, M.; Leclerc, C. Quiescence status of glioblastoma stem-like cells involves remodelling of Ca²⁺ signalling and mitochondrial shape. *Sci. Rep.* **2018**, *8*, 9731. [[CrossRef](#)]
39. Yang, C.; Tian, G.; Dajac, M.; Doty, A.; Wang, S.; Lee, J.-H.; Rahman, M.; Huang, J.; Reynolds, B.A.; Sarkisian, M.R.; et al. Slow-Cycling Cells in Glioblastoma: A Specific Population in the Cellular Mosaic of Cancer Stem Cells. *Cancers* **2022**, *14*, 1126. [[CrossRef](#)]
40. Antonica, F.; Santomaso, L.; Pernici, D.; Petrucci, L.; Aiello, G.; Cutarelli, A.; Conti, L.; Romanel, A.; Miele, E.; Tebaldi, T.; et al. A slow-cycling/quiescent cells subpopulation is involved in glioma invasiveness. *Nat. Commun.* **2022**, *13*, 4767. [[CrossRef](#)]
41. Wang, H.-H.; Liao, C.-C.; Chow, N.-H.; Huang, L.L.-H.; Chuang, J.-I.; Wei, K.-C.; Shin, J.-W. Whether CD44 is an applicable marker for glioma stem cells. *Am. J. Transl. Res.* **2017**, *9*, 4785–4806. [[PubMed](#)]
42. Wang, Z.; Zhang, H.; Xu, S.; Liu, Z.; Cheng, Q. The adaptive transition of glioblastoma stem cells and its implications on treatments. *Signal Transduct. Target. Ther.* **2021**, *6*, 124. [[CrossRef](#)] [[PubMed](#)]
43. Khan, A.B.; Lee, S.; Harmanci, A.S.; Patel, R.; Latha, K.; Yang, Y.; Marisetty, A.; Lee, H.-K.; Heimberger, A.B.; Fuller, G.N.; et al. CXCR4 expression is associated with proneural-to-mesenchymal transition in glioblastoma. *Int. J. Cancer* **2023**, *152*, 713–724. [[CrossRef](#)] [[PubMed](#)]
44. Sharma, P.; Aaroe, A.; Liang, J.; Puduvalli, V.K. Tumor microenvironment in glioblastoma: Current and emerging concepts. *Neurooncol Adv.* **2023**, *5*, vdad009. [[CrossRef](#)]
45. Zarodniuk, M.; Steele, A.; Lu, X.; Li, J.; Datta, M. CNS tumor stroma transcriptomics identify perivascular fibroblasts as predictors of immunotherapy resistance in glioblastoma patients. *NPJ Genom. Med.* **2023**, *8*, 35. [[CrossRef](#)]
46. Chugh, S.; Gnanapragassam, V.S.; Jain, M.; Rachagani, S.; Ponnusamy, M.P.; Batra, S.K. Pathobiological implications of mucin glycans in cancer: Sweet poison and novel targets. *Biochim. Biophys. Acta* **2015**, *1856*, 211–225. [[CrossRef](#)]
47. Sun, L.; Zhang, Y.; Li, W.; Zhang, J.; Zhang, Y. Mucin glycans: A target for cancer therapy. *Molecules* **2023**, *28*, 7033. [[CrossRef](#)]
48. Thomas, D.; Rathinavel, A.K.; Radhakrishnan, P. Altered glycosylation in cancer: A promising target for biomarkers and therapeutics. *Biochim. Biophys. Acta Rev. Cancer* **2021**, *1875*, 188464. [[CrossRef](#)]
49. Wan, Y.; Yu, L.-G. Expression and impact of c1galt1 in cancer development and progression. *Cancers* **2021**, *13*, 6305. [[CrossRef](#)]
50. Ju, T.; Aryal, R.P.; Kudelka, M.R.; Wang, Y.; Cummings, R.D. The Cosmc connection to the Tn antigen in cancer. *Cancer Biomark.* **2014**, *14*, 63–81. [[CrossRef](#)]
51. Brockhausen, I. Mucin-type O-glycans in human colon and breast cancer: Glycodynamics and functions. *EMBO Rep.* **2006**, *7*, 599–604. [[CrossRef](#)] [[PubMed](#)]
52. Guan, L.; Wang, W.; Ji, X.; Cheng, H.; Du, W.; Ye, L. T-antigen as a biomarker of progression-free survival in patients with glioblastoma. *Ann. Clin. Transl. Neurol.* **2024**, *11*, 1765–1774. [[CrossRef](#)] [[PubMed](#)]
53. Springer, G.F. T and Tn, general carcinoma autoantigens. *Science* **1984**, *224*, 1198–1206. [[CrossRef](#)]

54. Hofmann, B.T.; Schlüter, L.; Lange, P.; Mercanoglu, B.; Ewald, F.; Fölster, A.; Picksak, A.-S.; Harder, S.; El Gammal, A.T.; Grupp, K.; et al. COSMC knockdown mediated aberrant O-glycosylation promotes oncogenic properties in pancreatic cancer. *Mol. Cancer* **2015**, *14*, 109. [[CrossRef](#)]
55. Du, T.; Jia, X.; Dong, X.; Ru, X.; Li, L.; Wang, Y.; Liu, J.; Feng, G.; Wen, T. Cosmc Disruption-Mediated Aberrant O-glycosylation Suppresses Breast Cancer Cell Growth via Impairment of CD44. *Cancer Manag. Res.* **2020**, *12*, 511–522. [[CrossRef](#)]
56. Gao, T.; Du, T.; Hu, X.; Dong, X.; Li, L.; Wang, Y.; Liu, J.; Liu, L.; Gu, T.; Wen, T. Cosmc overexpression enhances malignancies in human colon cancer. *J. Cell. Mol. Med.* **2020**, *24*, 362–370. [[CrossRef](#)]
57. Thomas, D.; Sagar, S.; Caffrey, T.; Grandgenett, P.M.; Radhakrishnan, P. Truncated O-glycans promote epithelial-to-mesenchymal transition and stemness properties of pancreatic cancer cells. *J. Cell. Mol. Med.* **2019**, *23*, 6885–6896. [[CrossRef](#)]
58. Monzavi-Karbassi, B.; Pashov, A.; Kieber-Emmons, T. Tumor-Associated Glycans and Immune Surveillance. *Vaccines* **2013**, *1*, 174–203. [[CrossRef](#)]
59. Alves, I.; Fernandes, Â.; Santos-Pereira, B.; Azevedo, C.M.; Pinho, S.S. Glycans as a key factor in self and nonself discrimination: Impact on the breach of immune tolerance. *FEBS Lett.* **2022**, *596*, 1485–1502. [[CrossRef](#)]
60. Madsen, C.B.; Lavrsen, K.; Steentoft, C.; Vester-Christensen, M.B.; Clausen, H.; Wandall, H.H.; Pedersen, A.E. Glycan elongation beyond the mucin associated Tn antigen protects tumor cells from immune-mediated killing. *PLoS ONE* **2013**, *8*, e72413. [[CrossRef](#)]
61. Tseng, H.-C.; Inagaki, A.; Bui, V.T.; Cacalano, N.; Kasahara, N.; Man, Y.-G.; Jewett, A. Differential targeting of stem cells and differentiated glioblastomas by NK cells. *J. Cancer* **2015**, *6*, 866–876. [[CrossRef](#)] [[PubMed](#)]
62. Kozłowska, A.K.; Tseng, H.-C.; Kaur, K.; Topchyan, P.; Inagaki, A.; Bui, V.T.; Kasahara, N.; Cacalano, N.; Jewett, A. Resistance to cytotoxicity and sustained release of interleukin-6 and interleukin-8 in the presence of decreased interferon- γ after differentiation of glioblastoma by human natural killer cells. *Cancer Immunol. Immunother.* **2016**, *65*, 1085–1097. [[CrossRef](#)] [[PubMed](#)]
63. Poli, A.; Michel, T.; Thérésine, M.; Andrès, E.; Hentges, F.; Zimmer, J. CD56bright natural killer (NK) cells: An important NK cell subset. *Immunology* **2009**, *126*, 458–465. [[CrossRef](#)] [[PubMed](#)]
64. Nardy, A.F.F.R.; Freire-de-Lima, L.; Freire-de-Lima, C.G.; Morrot, A. The sweet side of immune evasion: Role of glycans in the mechanisms of cancer progression. *Front. Oncol.* **2016**, *6*, 54. [[CrossRef](#)]
65. Cornelissen, L.A.M.; Blanas, A.; Zaal, A.; van der Horst, J.C.; Kruijssen, L.J.W.; O’Toole, T.; van Kooyk, Y.; van Vliet, S.J. Tn antigen expression contributes to an immune suppressive microenvironment and drives tumor growth in colorectal cancer. *Front. Oncol.* **2020**, *10*, 1622. [[CrossRef](#)]
66. da Costa, V.; Mariño, K.V.; Rodríguez-Zraquia, S.A.; Festari, M.F.; Loes, P.; Costa, M.; Landeira, M.; Rabinovich, G.A.; van Vliet, S.J.; Freire, T. Lung Tumor Cells with Different Tn Antigen Expression Present Distinctive Immunomodulatory Properties. *Int. J. Mol. Sci.* **2022**, *23*, 12047. [[CrossRef](#)]
67. Quesnel, A.; Karagiannis, G.S.; Filippou, P.S. Extracellular proteolysis in glioblastoma progression and therapeutics. *Biochim. Biophys. Acta Rev. Cancer* **2020**, *1874*, 188428. [[CrossRef](#)]
68. Madzharova, E.; Sabino, F.; Kalogeropoulos, K.; Francavilla, C.; Auf dem Keller, U. Substrate O-glycosylation actively regulates extracellular proteolysis. *Protein Sci.* **2024**, *33*, e5128. [[CrossRef](#)]
69. Isavand, P.; Aghamiri, S.S.; Amin, R. Applications of Multimodal Artificial Intelligence in Non-Hodgkin Lymphoma B Cells. *Biomedicines* **2024**, *12*, 1753. [[CrossRef](#)]
70. Bowman, R.L.; Wang, Q.; Carro, A.; Verhaak, R.G.W.; Squatrito, M. GlioVis data portal for visualization and analysis of brain tumor expression datasets. *Neuro Oncol.* **2017**, *19*, 139–141. [[CrossRef](#)]
71. Bayin, N.S.; Frenster, J.D.; Kane, J.R.; Rubenstein, J.; Modrek, A.S.; Baitalmal, R.; Dolgalev, I.; Rudzenski, K.; Scarabottolo, L.; Crespi, D.; et al. GPR133 (ADGRD1), an adhesion G-protein-coupled receptor, is necessary for glioblastoma growth. *Oncogenesis* **2016**, *5*, e263. [[CrossRef](#)] [[PubMed](#)]
72. Zarkoob, H.; Taube, J.H.; Singh, S.K.; Mani, S.A.; Kohandel, M. Investigating the link between molecular subtypes of glioblastoma, epithelial-mesenchymal transition, and CD133 cell surface protein. *PLoS ONE* **2013**, *8*, e64169. [[CrossRef](#)] [[PubMed](#)]
73. Gabrusiewicz, K.; Rodriguez, B.; Wei, J.; Hashimoto, Y.; Healy, L.M.; Maiti, S.N.; Thomas, G.; Zhou, S.; Wang, Q.; Elakkad, A.; et al. Glioblastoma-infiltrated innate immune cells resemble M0 macrophage phenotype. *JCI Insight* **2016**, *1*, e85841. [[CrossRef](#)]
74. Goldman, M.J.; Craft, B.; Hastie, M.; Repečka, K.; McDade, F.; Kamath, A.; Banerjee, A.; Luo, Y.; Rogers, D.; Brooks, A.N.; et al. Visualizing and interpreting cancer genomics data via the Xena platform. *Nat. Biotechnol.* **2020**, *38*, 675–678. [[CrossRef](#)]
75. Tang, Z.; Li, C.; Kang, B.; Gao, G.; Li, C.; Zhang, Z. GEPIA: A web server for cancer and normal gene expression profiling and interactive analyses. *Nucleic Acids Res.* **2017**, *45*, W98–W102. [[CrossRef](#)]
76. Jain, S.; Rick, J.W.; Joshi, R.S.; Beniwal, A.; Spatz, J.; Gill, S.; Chang, A.C.-C.; Choudhary, N.; Nguyen, A.T.; Sudhir, S.; et al. Single-cell RNA sequencing and spatial transcriptomics reveal cancer-associated fibroblasts in glioblastoma with protumoral effects. *J. Clin. Investig.* **2023**, *133*, e147087. [[CrossRef](#)]
77. Hu, C.; Li, T.; Xu, Y.; Zhang, X.; Li, F.; Bai, J.; Chen, J.; Jiang, W.; Yang, K.; Ou, Q.; et al. CellMarker 2.0: An updated database of manually curated cell markers in human/mouse and web tools based on scRNA-seq data. *Nucleic Acids Res.* **2023**, *51*, D870–D876. [[CrossRef](#)]
78. Yoshihara, K.; Shahmoradgoli, M.; Martínez, E.; Vegesna, R.; Kim, H.; Torres-Garcia, W.; Treviño, V.; Shen, H.; Laird, P.W.; Levine, D.A.; et al. Inferring tumour purity and stromal and immune cell admixture from expression data. *Nat. Commun.* **2013**, *4*, 2612. [[CrossRef](#)]

-
79. Hänzelmann, S.; Castelo, R.; Guinney, J. GSVA: Gene set variation analysis for microarray and RNA-seq data. *BMC Bioinform.* **2013**, *14*, 7. [[CrossRef](#)]
 80. Liu, C.-J.; Hu, F.-F.; Xia, M.-X.; Han, L.; Zhang, Q.; Guo, A.-Y. GSCALite: A web server for gene set cancer analysis. *Bioinformatics* **2018**, *34*, 3771–3772. [[CrossRef](#)]

Disclaimer/Publisher’s Note: The statements, opinions and data contained in all publications are solely those of the individual author(s) and contributor(s) and not of MDPI and/or the editor(s). MDPI and/or the editor(s) disclaim responsibility for any injury to people or property resulting from any ideas, methods, instructions or products referred to in the content.